Biochimica et Biophysica Acta 1853 (2015) 646–659

Contents lists available at ScienceDirect

Biochimica et Biophysica Acta

journal homepage: www.elsevier.com/locate/bbamcr

The giardial ENTH protein participates in lysosomal protein trafficking and endocytosis

Constanza Feliziani [a], Nahuel Zamponi [a], Natalia Gottig [b], Andrea S. Rópolo [a], Adriana Lanfredi-Rangel [c], Maria C. Touz [a,*]

[a] Instituto de Investigación Médica Mercedes y Martín Ferreyra, INIMEC, CONICET, Universidad Nacional de Córdoba, Friuli 2434, Córdoba, Argentina
[b] Molecular Biology Division, Facultad de Ciencias Bioquímicas y Farmacéuticas, Instituto de Biología Molecular y Celular de Rosario, CONICET, Universidad Nacional de Rosario, Rosario, Argentina
[c] Serviço de Microscopia Eletrônica, Centro de Pesquisas Gonçalo Moniz, FIOCRUZ-BA, Brazil

ARTICLE INFO

Article history:
Received 5 September 2014
Received in revised form 18 December 2014
Accepted 30 December 2014
Available online 6 January 2015

Keywords:
ENTH motif
Lysosome
Endosome
Giardia lamblia

ABSTRACT

In the protozoa parasite *Giardia lamblia*, endocytosis and lysosomal protein trafficking are vital parasite-specific processes that involve the action of the adaptor complexes AP-1 and AP-2 and clathrin. In this work, we have identified a single gene in *Giardia* encoding a protein containing an ENTH domain that defines monomeric adaptor proteins of the epsin family. This domain is present in the epsin or epsin-related (epsinR) adaptor proteins, which are implicated in endocytosis and Golgi-to-endosome protein trafficking, respectively, in other eukaryotic cells. We found that GlENTHp (for *G. lamblia* ENTH protein) localized in the cytosol, strongly interacted with $PI3,4,5P_3$, was associated with the alpha subunit of AP-2, clathrin and ubiquitin and was involved in receptor-mediated endocytosis. It also bonded PI4P, the gamma subunit of AP-1 and was implicated in ER-to-PV trafficking. Alteration of the GlENTHp function severely affected trophozoite growth showing an unusual accumulation of dense material in the lysosome-like peripheral vacuoles (PVs), indicating that GlENTHp might be implicated in the maintenance of PV homeostasis. In this study, we showed evidence suggesting that GlENTHp might function as a monomeric adaptor protein supporting the findings of other group indicating that GlENTHp might be placed at the beginning of the ENTH family.

1. Introduction

Eukaryotic cells have to deal with the fact that, after translation at the ribosomes, most proteins must be specifically targeted to the organelle in which they must function. As cellular components became more complex and abundant during evolution, subcellular compartmentalization developed into an essential feature to prevent the inappropriate meeting of certain intracellular components and facilitate efficient ordered reactions [1]. In eukaryotes, lipids and proteins synthesized in the endoplasmic reticulum (ER) reach their intended organelle, with the Golgi complex being the major sorting point in the secretory pathway. Among the intracellular compartments, endosomes and lysosomes are part of the cell's central system, playing multifunctional roles in the process of phagocytosis, autophagy, endocytosis, recycling, and degradation [2, 3]. To maintain these compartments, cells have evolved mechanisms to ensure that specific proteins are delivered to specific organelles. In this scenario, the parasite *Giardia lamblia* is distantly related to the well-studied model organisms of animals and fungi, and is thus a tractable organism from which to compare function across deep evolutionary time. *Giardia* trophozoites lack the organelles involved in intracellular protein trafficking and secretion in most types of eukaryotic cells, such as the traditional Golgi apparatus and the typical endosomal/lysosomal system. Instead, the Golgi function seems to be performed by the ER [4], while the function of the endosomal–lysosomal system is achieved by peripheral vacuoles (PVs), which are one of the most unusual organelles among the eukaryotes because they fulfill both endosomal and lysosomal functions (reviewed in [5]).

PVs are highly polarized vacuoles localized just below the plasma membrane of trophozoites and have been observed occasionally between the nuclei [6–8]. When first described, PVs were proposed as lysosome-like vacuoles and later also as a simple system for uptake of extracellular material by fluid-phase [9, 10]. From there, it became increasingly clear that the nature of PVs and the machinery involved in protein trafficking to and from these organelles are unique and encompass conserved features and particular characteristics. Unlike the distinct but connected network involving early/late/recycling endosomes, multivesicular bodies and lysosomes, the primary functions of which are well-distinguished, PVs bring together the sorting of internalized cargo, recycling and degradation functions all-in-one [4, 6, 11–13].

It is not surprising then that the molecules that participate in the maintenance of PV homeostasis and function preserve some features

* Corresponding author at: Instituto de Investigación Médica Mercedes y Martín Ferreyra, INIMEC, CONICET, Universidad Nacional de Cordoba, Friuli 2434, 5000, Córdoba, Argentina. Tel.: +54 351 468 1465; fax: +54 351 4695163.
E-mail address: ctouz@immf.uncor.edu (M.C. Touz).

http://dx.doi.org/10.1016/j.bbamcr.2014.12.034
0167-4889/

but contain particularities. For instance, in mammalian cells, the role of clathrin and adaptor protein complexes (AP) in endosomal and lysosomal protein delivery involves the participation of four tetrameric adaptor proteins (AP-1 to -4) and an increasing number of monomeric adaptors. Previously, we showed that the soluble hydrolase acid phosphatase (AcPh) is transported to the PVs by a receptor via AP-1 [14]. On the other hand, giardial AP-2 participates in receptor-mediated endocytosis and is crucial in the internalization of lipoproteins in *Giardia* [7]. The existence of a giardial clathrin heavy chain [15], and the absence of other adaptor complexes including AP-3 and AP-4, the monomeric adaptor GGA, Dab2, or Hrs [16], supports the hypothesis that this parasite utilizes a conserved but highly reduced set of proteins compared with the more complex machinery for endosomal–lysosomal trafficking present in other eukaryotes.

However, when we extended our focus to other molecules involved in lysosomal-protein trafficking and PV homeostasis, we found a single gene encoding an ENTH domain-containing epsin-related protein (*Giardia lamblia* ENTH protein, GlENTHp) observed in the monomeric adaptors epsin or epsinR, which we exploited as an opportunity for functional analysis in an evolutionary context. In mammalian cells, this domain is a conserved membrane-interacting module present at the NH2-terminus of proteins that often contains consensus sequences for binding to clathrin coat components and their accessory factors at the C-terminus (Fig. 1A) [17]. The C-terminal domain of epsin1–3 harbors several specific sequence motifs that bind to clathrin, αAP-2 and Eps15 [18]. The ENTH domain binds to the polyphosphoinositides (PIs) $PI4,5P_2$ and induces membrane curvature [19]. Epsin also contains ubiquitin-interaction motifs (UIMs) that interact with polyubiquitins and may capture ubiquitinated cargo receptors for internalization [20–22]. Epsin 1 is localized to clathrin-coated pits, and disruption of its interactions with other endocytic proteins blocks clathrin-mediated endocytosis [23]. EpsinR, on the other hand, is a clathrin sorting-associated protein that binds to PI4P, clathrin, GGAs and the gamma appendage domain of AP-1. In these cells, its distribution overlaps with the perinuclear pool of clathrin and AP-1 adaptors [24, 25]. Unlike epsins involved in coated pit formation at the plasma membrane, epsinR is strongly enriched in clathrin-coated vesicles and is associated with Golgi-to-endosome trafficking [24].

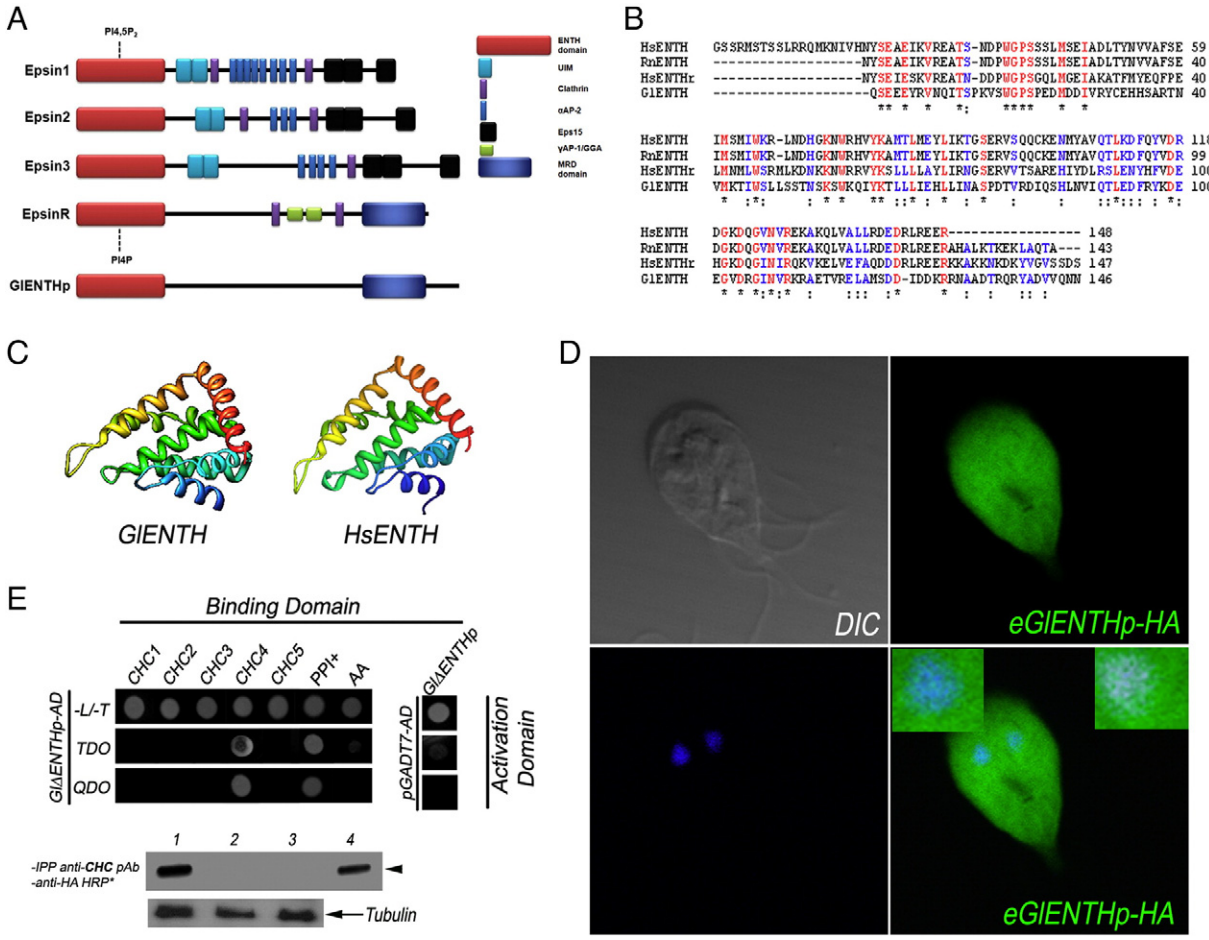

Fig. 1. *Giardia* possesses an ENTH protein. (A) Schematic representation of epsins 1–3, epsinR proteins and GlENTHp. These proteins share a similar modular organization, with a N-terminal ENTH domain that interacts with PIs and a C-terminal domain containing motifs for interaction with a variety of binding partners. EpsinR contains a methionine-rich sequence with a not yet clearly defined function. Besides the ENTH domain and the N-terminus, GlENTHp also possesses a methionine-rich sequence also enriched in proline and glutamine. (B) Amino acid sequence alignment of the ENTH motif of human epsin (HsENTH), rat epsin (RnENTH), human epsinR (HsENTHr) and *Giardia* ENTH (GlENTH) is shown. Strictly conserved residues are highlighted in red and asterisks (*) while conserved amino acids in at least 2 out of 4 sequences are shown in blue and colons (:). (C) Ribbon diagram of the ENTH domain of *Giardia* and human epsin. The ENTH domains display an all α-helical structure and are composed of 7 α-helices. (D) eGlENTHp-HA (green) mainly localized in the cytoplasm but also inside the nuclei (blue) in *e-ehthp-ha* transgenic trophozoites. DAPI (diamidino-2-phenylindole) was used to stain the nuclei. Colocalization areas between green and DAPI are depicted in cyan in the insets. Differential interference contrast (DIC) microscopy is shown as insets. Images were acquired with confocal laser-scanning fluorescence microscopy. Bar, 5 μm. (E) YTH assays show that GlΔENTHp strongly interacts with the aa sequence CHC4 of giardial clathrin heavy chain (colonies growing in TDO and QDO selective mediums). +PPI: Positive protein–protein interaction control. AA: Autoactivation negative control. Autoactivation control also includes the pair **p**GlΔENTHp-BD and the empty pGADT7 vectors (right panels). Co-immunoprecipitation confirms that GlENTHp interacts with clathrin in vivo (bottom panel). 1: GlENTHp-HA was immunoprecipitated from transgenic cells using an anti-clathrin pAb. GlENTHp-HA (~50 kDa band, arrowhead) was detected by using HRP-labeled anti-HA mAb. 2: control using an irrelevant pAb. 3: control using untransfected cells. 4: Input lane. An aliquot of total cell lysate before immunoprecipitation for tubulin was used as a loading control. These data show representative blots from one of the three independent experiments.

When the ENTH protein family is analyzed in an evolutionary context, it was suggested that the Human Epsin1–3 and yeast Ent1–2, which are required for endocytosis, are specific to Opisthokonta (Metazoa and Fungi) and that this subfamily was acquired more recently probably by duplication of the epsinR [26, 27]. In these studies, the phylogenetic analysis of GlENTHp exposed its epsinR characteristics, supporting the concept that epsinR (or ENTHA) is the origin of the family. In this paper, we investigate the function of GlENTHp and present some evidence showing that it might function as a monomeric adaptor protein. Future work will reveal whether GlENTHp is the epsin-like adaptor from which all the family evolves.

2. Materials and methods

2.1. Ethics statement

The animals (BALB/c mice) were bred and maintained at the vivarium of the Instituto Mercedes & Martin Ferreyra (INIMEC-CONICET-UNC) that have been inspected and approved by the Department of Animal Care (SENASA) from Argentina. Animal maintenance and care followed the general guidelines provided by the National Institutes of Health of the U.S.A.

2.2. Sequence analysis and 3D model prediction

Signal peptide prediction was performed by using the following programs and web servers: Phobius (http://phobius.sbc.su.se/) [28], SignalP 4.1 (http://www.cbs.dtu.dk/services/SignalP-4.1/) [29] and PSORT II (http://www.psort.org/) [30]. Homology searches were performed online with Blastp at http://www.ncbi.nlm.nih.gov/blast/Blast.cgi. Multiple sequence alignment was performed using the CLUSTAL 2.1 program [31]. Amino acid sequences of proteins with an ENTH domain were gathered for *Homo sapiens* (Hs), *Rattus norvegicus* (Rn), the protists *G. lamblia* (Gl), *Plasmodium falciparum* (Pf), *Trypanosoma cruzi* (Tc), *Trypanosoma brucei* (Tb), *Leishmania major* (Lm), *Toxoplasma gondii* (Tg),, *Cryptosporidium parvum* (Cp), *Trichomona vaginalis* (Tv), and *Spironucleus salmonicida* (Ss) and the single-cell green alga *Chlamydomonas reinhardtii* (Cr), from the NCBI. 3D was performed with the Max Planck Institute Bioinformatics Toolkit, or Hidden Markov Models (HHPred-available at http://protevo.eb.tuebingen.mpg.de/toolkit/), which uses Modeller v7.7 for predictive modeling. MolMol [32] was used to create 3D images. The validation of the predicted 3D structures was performed with ANOLEA [33], Verify 3D [34], and MolProbity [35]. The ENTH domain of GlENTHp was constructed using the ENTH domain from human epsin (HsENTH) as a model. HsENTH bound to $PI4,5P_2$, as dissolved by X-ray diffraction (resolution: 1.70 A°) (Swiss-Model repository, UniProt AC: Q9Y6I3). The SNAP (screening for non-acceptable polymorphisms) method (https://www.rostlab.org/services/SNAP/) was used to predict the functional effects of single amino acid substitutions [36].

2.3. Antibodies and other reagents

Anti-ubiquitin polyclonal antibody specific for *G. lamblia* ubiquitin was a gift of Dr. Moises Wasserman [37]. Anti-HA, anti-Tubulin, HRP-labeled anti-HA, FITC-labeled, and TexasRed-labeled anti-HA mAbs were purchased from Sigma (St. Louis, MO). 9C9 mAb was employed to detect the ER-BiP (immunoglobulin heavy chain-binding protein) [38]. Anti-μ2 mAb 2 F5 was used for the μ2 subunit of AP2 [7]. Alexa Fluor 555 was used for the primary antibody label (Zenon Tricolor Mouse IgG1 Labeling Kit, Molecular Probes, Invitrogen). Both BODIPY-labeled LDL and LysoTracker Red DND-99 were purchased from Molecular Probes-Invitrogen. The 20 kDa FITC-dextran was purchased from sigma (St. Louis, MO). Fluorescein (FITC) conjugated anti-$PI3,4,5P_3$ and purified anti PI4P antibody Mouse Monoclonal IgM was purchased from Echelon Biosciences Inc.

2.4. Giardia cell lines and vectors

Trophozoites of the isolate WB, clone 1267 [39], were cultured in TYI-S-33 medium supplemented with 10% adult bovine serum and 0.5 mg/ml bovine bile, as previously described [40]. These trophozoites were used as hosts for the expression of transgenic genes and as non-transfected controls. The GlENTHp open reading frame was amplified from genomic DNA using the f1 (CATTCCATGGCTGCGAAGGAGAACAT GCAG) and r1 (CATTGTATACAAAGAAGGACATGAGGTCGG) primers and cloned into the plasmid **p**TubHAc-pac [41] to generate the **p**GlENTHp-HA episomal vector. To express the endogenous GlENTHp, the **p**eGlENTH-HA vector was constructed by replacing the tubulin promoter of the **p**GlENTHp-HA vector by a sequence containing the putative *glenthp* endogenous promoter using the primers f2 (5′CATTAAGC TTCATATAAGCTCTTCGGC) and r2 (5′ CATTCCATGGTTTTTTTCAACCAT ATTTGT). The ENTH domain of GlENTHp was mutated in the K75 to A75 by site-mutation using the **p**GlENTHp-HA vector and the f3 (TCTG GTCACTTCTTTCAAGCACCAACTCAGCTAGCTGGAAGCAGATC) and the r3 (GATCTGCTTCCAGCTAGCTGAGTTGGTGCTTGAAAGAAGTGACCAGA) primers [18] to generate **p**$GlENTH_{K75A}$p-HA. All vectors contained a puromycin cassette under the control of the endogenous non-regulated glutamate dehydrogenase (*gdh*) promoter for cell selection (Fig. S1A). Stable episomal trophozoite transfection was performed as previously described [14, 42–45] except for **p**eGlENTHp vector, which was cut with *Not*I to produce stable integrated transfectans (Fig. S1B). Drug-resistant trophozoites were usually apparent by 7–10 days post-transfection.

2.5. Immunofluorescence assay (IFA)

Trophozoites were washed with PBSm (1% growth medium in PBS, pH 7.4) and allowed to attach themselves to slides at 37 °C. After fixation with 4% formaldehyde, the cells were washed and blocked with PBS containing 10% normal goat serum and 0.1% Triton X-100. The cells were then incubated with specific Abs in PBS containing 3% normal goat serum and 0.1% Triton-X100, followed by incubation with FITC-conjugated goat anti-mouse secondary antibody. For direct double staining, the anti-HA mAb (Sigma, St. Louis, MO) was labeled with Zenon Alexa Fluor 488 and was used to detect HA-tagged GlENTHp (final dilution of anti-HA 1:500), while 9C9 and 2 F5 mAbs were labeled with Zenon Alexa Fluor 555 (1:200 final dilution), following the suggested protocol (Zenon Tricolor Mouse IgG_1 Labeling Kit, Molecular Probes, Invitrogen Corporation, Carlsbad, CA). Controls included the omission of the primary antibody and the staining of *wild-type* cells. Finally, preparations were washed and mounted in Vectashield mounting medium. Fluorescence staining was visualized with a motorized FV1000 Olympus confocal microscope (Olympus UK Ltd, UK), using 63× or 100× oil immersion objectives (NA 1.32, zoom X). The fluorochromes were excited using an argon laser at 488 nm and a krypton laser at 568 nm. DAPI was excited with ultraviolet light using a 364 nm Argon laser. Detector slits were configured to minimize any cross-talk between the channels. Differential interference contrast images were collected simultaneously with the fluorescence images, by the use of a transmitted light detector. Images were processed using FV10-ASW 1.4 Viewer and Adobe Photoshop 8.0 (Adobe Systems) software. The colocalization and deconvolution were performed using MetaMorph software (Molecular Devices, Silicon Valley, CA). Fluorescent images were observed with an inverted microscope (Carl Zeiss Axiovert 35 M) equipped with epifluorescence and differential interference contrast (DIC) optics using a 100× oil immersion objective (Carl Zeiss) and were captured under regular fluorescence microscopy with a silicon-intensified target camera (SIT-C2400; Hamamatsu Phototonics, Bridgewater, NJ). The images were digitized directly into a Metamorph/Metafluor Image Processor (Universal Imaging Corporation, West Chester, PA).

2.6. Generation of a polyclonal antibody against GlCLH

A fragment that codifies *Giardia* clathrin heavy chain (GlCHC) N-terminus (from 1 to 404 aa) was cloned in a pET32a vector (Novagen). The construct was transformed into *E. coli* strain BL21 (pLysS), and the synthesis of recombinant protein fusioned at its N-terminus with a thioredoxin tag was induced by addition of 0.5 mM isopropyl-b-Dthiogalactopyranoside (IPTG) for 3 h at 25 °C. The recombinant protein was purified by affinity chromatography from the soluble fraction of the bacterial lysate using Ni^{2+}-nitrilotriacetate (Ni-NTA) agarose (Qiagen, Hilden, Germany), and checked by sodium dodecylsulphatepolyacrylamide gel electrophoresis (SDS-PAGE). After protein purification the thioredoxin tag was deleted with thrombin and the purified clathrin N-terminus was used as immunogen. GlCHC fusion protein (100 μg) was emulsified in TiterMax adjuvant (SIGMA) and used to subcutaneously immunize BALB/c mice. Mice were boosted subcutaneously after 21 days with 200 μg of the same preparation and 20 days later boosted again intravenously with 100 μg of the antigen suspended in PBS. To test the production of anti-GlCHC positive polyclonal antibodies (pAb), sera of three immunized mice were analyzed by IFA and immunoblotting (Fig. S2).

2.7. Yeast-two hybrid (YTH) assay

The MATCHMAKER Two-Hybrid System was used following the manufacturer's recommended protocol (Clontech, Palo Alto, CA). The two-hybrid pGADT7-Rec(LEU2) vector (GAL4 transcription activation domain; AD) containing the sequences for glENTHp or glΔENTHp (lacking the ENTH domain sequence) were used as bait, while γap-1, *αap-2*,*μap-1*, *μap-2*, *ubiquitin* genes and *glchc* gene fragments (see results section) were inserted into the pGBKT7(TRP1) vector (GAL4 DNA binding domain; BD). The AH109 transformants were cultured at 30 °C for 4–5 days on plates with minimal medium lacking leucine and tryptophan (−L/−T) to test for positive transformation, or in the absence of leucine, tryptophan, and histidine (TDO, triple dropout medium) to study specific protein interactions, as previously described [14]. High-stringency medium that lacked adenine (QDO) was also used to test strong protein-protein interactions. In all the assays presented, the control of positive interaction (pESCP-AD/pμ1-BD, protein–protein interaction control, PPI+) [41] and the negative controls (**p**GlΔ_{ENTH}p-AD/**p**GBKT7, autoactivation, AA) or **p**GADT7/**p**GlΔ_{ENTH}p-BD were included.

2.8. Immunoprecipitation (IPP) assay

Wild-type or *glenth-ha* trophozoites were harvested and suspended in 500 μl of lysis buffer (50 mM NaH_2PO4, 300 mM NaCl, 1% Triton X-100, and Complete protease inhibitors—Roche-) for 1 h at 4 °C. After mild sonication using a Branson sonifier 250 (Branson, CT) with an output control of 4 and a 30% duty cycle (sonication complex), the lysate was centrifuged at 10,000 rpm for 10 min at 4 °C, and the supernatant mixed with anti-CHC or anti-ubiquitin pAb and incubated overnight at 4 °C. Protein A-G-agarose beads (30 μl; Qiagen, Valencia, CA) were added to each sample and incubated for 4 h at 4 °C. Beads were pelleted at 2500 rpm for 5 min and washed four times with washing buffer (50 mM NaH_2PO_4, pH 8.0; 300 mM NaCl; 0.1% Triton X-100; and protease inhibitors). Beads were re-suspended in sample buffer and boiled for 10 min before immunoblot analysis using HRP-labeled anti-HA mAb. Immunoprecipitation using anti-PIs mAbs was performed as described by Li and Russell [46]. Briefly, *glenth-ha* and *glenthk75a* transgenic trophozoites were first stimulated by addition of 0.62% bovine bile (Sigma-Aldrich) and incubated at 37 °C for 15 min. Stimulation was stopped by the addition of cold KRT buffer and the cells centrifuged at 5000 *g* in a refrigerated microcentrifuge at 4 °C for 15 min [47, 48; Gesumaria and Machado, personal communication]. After lysis, the cells were exposed to 5 μl of anti-PI3,4,5P_3 or anti-PI4P IgM mAbs and Protein L-agarose beads, and the technique accomplished as above. Finally, the resulted samples were tested by immunoblotting using HRP-labeled anti-HA mAb to reveal the presence of GlENTHp-HA and $GlENTH_{K75A}$-HA.

2.9. Phospholipid binding

Protein binding to phospholipids was investigated in a protein lipid overlay assay using PIP Strips™ (Echelon Biosciences Incorporated) according to the manufacturer's protocol. In brief, the membrane was blocked in PBS-T (0.1% v/v Tween-20) + 3% BSA for 1 h at RT. *glenth-ha* and *glenthk75a* transgenic parasites were lysed using PBS-T + 3% BSA and mild sonication, following the protocol suggested by the company (Echelon Biosciences, PIP Strips). 0.5 μg/ml of total proteins from each lysate in PBS-T + 3% BSA were added to nitrocellulose membrane and incubated for 5 h at RT. The membrane was washed three times for 10 min in PBS-T. GlENTHp-HA and $GlENTH_{K75A}$p-HA were detected by incubation with a 1:1000 dilution of anti-HA mAb in PBS-T + 3% BSA, followed by incubation with anti–mouse HRP conjugate (Abcam) in a 1:2000 dilution and by ECL (Amersham Biosciences). The recombinant GST-tagged PLC-δ1 PH domain protein that binds to PI4,5P_2 was used as a positive control while lysate of *wild-type* trophozoites was used as negative control.

2.10. Subcellular fractionation

Trophozoites were grown to logarithmic phase and washed twice in PBS, resuspended in cold hypotonic lysis buffer (10 mM Tris–HCl, pH 7.5 plus protease inhibitors) and then incubated on ice for 5 min. The cell lysate was centrifuged in a refrigerate microfuge at 16,000 *g* at 4 °C for 10 min. The pellet fraction was washed once with cold hypotonic lysis buffer, resuspended in sample buffer and incubated on ice for 25 min prior to taking for SDS-PAGE. Equivalent amounts of cytoplasmic (C) and membrane (M) fractions were analyzed by immunoblotting [26]. Gel-pro Analyzer 4.5 software was used to obtain quantitative information from blots (Media Cybernetics, Inc. Rockville, MD, USA). Five membranes for each sample were quantified.

2.11. PI3,4,5P_3 and PI4P subcellular localization

Growing trophozoites were first stimulated by addition of 0.62% bovine bile as described above (Immunoprecipitation 2.9). For IFA the fixed cells were permeabilized with 0.5% saponin (Sigma) at RT for 15 min and the Ab anti-PI3,4,5P_3 and anti-PI4P were added at a 1:50 and 1:200 dilution, respectively. TBS buffer was used in all steps.

2.12. GlENTHp downregulation

To silence the GlENTHp, nucleotides 1–778 from the 1218 nt of *glenth* were introduced into the dsRNA vector [14, 49], following PCR amplification using the dsRNA *gENTHp*F (**a**): 5′-*CATTGGATCCCCTGCGAA GGAGAACATGCA*-3′ and dsRNA *gENTHp*R (**a′**): 5′-*CATTGCATGCCCATAC CCATGCCCATGTTG*-3′ primers. 10 μg of the resulting **p**ds-glenth vector (Fig. S1B) was used to transfect the *Giardia* clone WB1267 as described above. After 48 h of Tet induction (10 μg/ml, final concentration), dsRNA production as well as *GlENTHp* depletion (by detection of the 440-3′ nt of *glenth*) were confirmed by qRT-PCR before performing analysis of cell growth.

2.13. Real-time PCR

Cultured *wild-type* and transgenic trophozoites were homogenized in Trizol reagent (Invitrogen Life Technologies) and stored at −80 °C before total RNA extractions, according to the manufacturer's protocol. RNA was treated with DNase (Promega) before determination of nucleic

acid concentration and cDNA synthesis with RevertAid™ Reverse Transcriptase (Fermentas). cDNA was analyzed for *wild-type* and transgenic trophozoites genes using real-time PCR SYBR Green Master Mix from Invitrogen (Invitrogen Life Technologies, Carlsbad, USA) single stranded cDNA (100 ng of the input total RNA equivalent), and 800 nM of amplification primer were used in a reaction volume of 20 μl. The primer set GlENTHpRealFw: 5′-CGGTTCATCAGCCCACTCAT-3′ and GlENTHpRealRv v: 5′-CGTCTGGGCTGGAGCTTGT-3′ primers, used to amplify the *glenth* nt sequence from 344 to 405, were designed using Primer Express software (Applied Biosystems). Runs were performed on a 7500 standard system (Applied Biosystems, USA). The relative-quantitative RT-PCR conditions were: 50 °C for 2 min, 95 °C 10 min and 40 cycles at 95 °C for 15 s and 60 °C for 1 min. Gene expression was normalized to the housekeeping gene *gdh* (f: 5′AGGGCGGCTCCGACTTT3′ and r: 5′AGCG CATGACCTCGTTGTC3′ primers) and calculated using the ΔΔCt method. Melt curve analyses were performed to ensure the specificity of the qPCR product. Statistical analysis was carried out using GraphPad Prism software (GraphPad Software, Inc.). The *t*-test was used to determine differences between *wild type* cells (control group) and *glenth-ha* cells, *glenthk75a* and *ds-glenth* transgenic cells.

2.14. Uptake experiments

To analyze the role of GlENTHp in endocytosis, either 20,000 Da FITC-dextran or BODIPY-LDL was used as an endocytic marker to study fluid phase or receptor-mediated endocytosis mechanisms, respectively [7]. The trophozoites transfected with the **p**GlENTHp-HA, **p**GlENTH$_{K75A}$p-HA or **p**ds-GlENTH vectors and *wild-type* trophozoites were cultured until the logarithmic phase and the uptake experiments were performed as described [7, 12]. Briefly, the growth medium was exchanged for labeling buffer (50 mM glucose, 10 mM cysteine, 2 mM ascorbic acid in PBS, pH 7.1) containing 7.5 μg of BODIPY-labeled LDL. After 30 min at 37 °C, the trophozoites were visualized by living fluorescence microscopy. Controls for this experiment included the addition of FITC-dextran to *wild-type* and transgenic trophozoites. The number of cells showing PV localization of the fluorescent dye was quantified in each sample. The Fiji image processing package (http://fiji.sc/wiki/index.php/Fiji) was used to analyze fluorescent images. Statistical calculations were performed using the R software environment http://www.r-project.org. Data were expressed in percentage of PV-labeled cells to all counted cells. All images were equally processed. The most representative effect for each type of cells is shown.

2.15. Acid phosphatase activity assay

ELF97 (Molecular Probes; Eugene, OR) was used to test acid phosphatase activity, as previously [6]. Briefly, *wild-type*, *glenth-ha*, *glenthk75a*, and *ds-glenth* trophozoites were incubated with 20 μM ELF97 for 15 min and ELF97 substrate in 110 mM acetate buffer (pH 5.5), containing 1.1 mM sodium nitrite added later. No cell membrane permeabilization step was needed for the ELF97 staining. The fluorescence signal was analyzed and documented by conventional fluorescence microscopy, using a 364 nm Argon laser (Carl Zeiss Axiovert 35 M) and captured with a silicon-intensified target camera (SIT-C2400; Hamamatsu Phototonics, Bridgewater, NJ). Total ELF97 stained area was quantified in each independent cell. For quantitative studies, the brightness of the fluorescence emission from a defined area was measured using the Fiji image processing package (http://fiji.sc/wiki/index.php/Fiji). Statistical calculations were performed using the R software environment http://www.r-project.org. At least 50 cells were assessed three times per condition.

2.16. Transmission electron microscopy (TEM)

Wild-type trophozoites, *glenthp-ha*, *glenthk75ap* and *ds-glenth* transgenic trophozoites were twice washed with PBS at 37 °C and then fixed when still adhered to culture tubes in a solution containing 2.5% glutaraldehyde, 4% freshly prepared formaldehyde, and 5 mM CaCl2 in 0.1 M cacodylate buffer or PHEM buffer, pH 7.2, plus 4% sucrose. Then the cells were scraped off the tube wall with a rubber policeman, washed in buffer, and postfixed for 60 min at 4 °C in a solution containing 1% osmium tetroxide, 0.8% potassium ferrocyanide in 0.1 M cacodylate buffer. Subsequently, the cells were washed in buffer, dehydrated in acetone, and embedded in Epon. Thin sections were stained with uranyl acetate and lead citrate and observed in a Zeiss 109 electron microscope. All available TEM images were quantified.

2.17. Growth curves

For the growth curves, tubes containing 7 ml of growth medium without puromycin were inoculated with 1.8×10^4 trophozoites from *wild-type*, *glenthp-ha*, *glenthk75ap* or *ds-glenth* logarithmic phase cultures. Tetracycline (10 μg/ml, final concentration) was added to *wild-type* and *ds-glenth* to test the effect of Tet and GlENTHp depletion in trophozoite growth, respectively. Every 12 h, the tubes were chilled on ice for 20 min to detach adherent living trophozoites and the number of viable cells was determined by counting on a hemocytometer after staining with 0.4% Trypan blue according to instructions from the manufacturer (Sigma Chemical Co, USA). A comparison of means was performed using the Independent-Samples Student's *t*-test from the SSPS Statistic program. $p \leq 0.05$ was considered significant.

2.18. PI3K inhibition

W*ild-type*, *glenth-ha* and *glenthk75a* trophozoites were grown for 48 h prior to treatment with PI3K inhibitor LY294002 (2-(4-Morpholinyl)-8-phenyl-4H-1-benzopryan-4-one hydrochloride) (SIGMA). Cells were treated overnight with different concentrations of LY294002 from 100× stock solution in DMSO. Significant amount of healthy cells were observed at the concentration of 30 μM of LY294002 [50]. Control cells were treated with equal volumes of DMSO. Experiments were carried out in triplicate. Trophozoites were fixed in 4% paraformaldehyde (Sigma) and processed as described above.

3. Results

3.1. Characterization of the ENTH protein in Giardia

The clathrin-mediated specific enzyme transport to the PVs has to be made with the participation of mediator proteins, like the monomeric or tetrameric APs. Searching the *Giardia* genome database (GiardiaDB http://giardiadb.org/giardiadb/), we found a sequence presenting an ENTH domain (GL50803_3256), which defines monomeric adaptor proteins of the epsin family (Fig. 1A–C). Sequence comparisons of the *G. lamblia* ENTH domain (GlENTH) with others of the epsin and epsinR proteins showed that it shares ~25% sequence identity with the ENTH of *H. sapiens* epsin (HsENTH), ~31% sequence identity with the ENTH of *H. sapiens* EpsinR, and ~30% sequence identity with the ENTH of *R. norvegicus* (RnENTH) epsin (Fig. 1B). When the tertiary structure of the ENTH domain was analyzed, an α-helical structure composed of 7 α-helices was depicted with 100% homology with the structure of the ENTH domain from epsin1 of human (*H. sapiens* HsENTH) (Fig. 1C) and rat (not shown). Comparison of ENTH domain of *Giardia* with the ones described in other early branching eukaryotes showed degrees of sequence conservation similar to those found between GlENTH and the ENTH domain from human and rat (27% on average) (Fig. S3A–B).

Immunofluorescence assay and confocal microscopy showed that most of eGlENTHp-HA, expressed under its endogenous promoter, was found in the cytosol but it was also present inside the nuclei (Fig. 1D and Fig. S1) and, by performing yeast two hybrid (YTH) and co-immunoprecipitation assays, we showed that GlENTHp was able to interact with the clathrin heavy chain (CHC) (Fig. 1E) suggesting that

GlENTHp might be a clathrin-associated sorting protein. In the YTH assays, GlΔENTHp (which lacks the ENTH domain but conserved the C-terminus domain) was cloned into the vector holding the transcription activation domain (AD) as bait and confronted with the 5616 nt-clathrin sequence divided into 5 fragments (CHC1: 1–1200 nt, CHC2: 1200–2400 nt, CHC3: 2400–3600 nt, CHC4: 3600–4995 nt, and CHC5: 4995–5616 nt), cloned into a vector containing the DNA binding domain (BD). Colony growth assays showed that one clathrin binding domain (CHC4) strongly interacted with GlΔENTHp, as indicated by the growth in the restricted medium TDO and QDO (see Materials and methods section). No interactions were observed for the CHC1, CHC2, CHC3, or CHC5 prey protein sequences, indicating that the CHC4–Gl ΔENTHp interaction is specific (Fig. 1E, upper panels). The same results were observed using GlENTHp (not shown). The interaction between GlENTHp-HA and clathrin was confirmed to be specific by in vivo co-immunoprecipitation assays. GlENTHp-HA from transgenic *Giardia* lysates was pulled down by anti-CHC mouse pAb immobilized on protein L-agarose beads (Fig. 1E, bottom panel). This interaction appears specific, as no GlENTHp-HA could be detected in the control using a non-related Ab (Ctrol1) or control without antibody (Ctrol2) (Fig. 1E, bottom panel).

3.2. Giardial ENTH domain binds inositol phospholipids

The critically important feature of epsin is the evolutionary conserved ENTH domain, which binds PIs that are differentially enriched in cellular membranes. The phospholipid interaction mediated by the ENTH domain of the classical epsins and of epsinR has different lipid specificity, with epsin showing preference for $PI4,5P_2$ of the plasma membrane, and epsinR for PI4P enriched in membranes of the Golgi and cytoplasmic vesicles [51]. It was shown that mutation of the conserved residue K76 (K75 in GlENTHp) appeared to be involved in the direct binding of the ENTH domain to PIs in mammalian cells and *Dictyostelium* [18, 52]. Thus, to test the ability of GlENTHp-HA to bind acidic phospholipids, we produced a mutant $GlENTH_{K75A}$p-HA, in which K75 of the ENTH domain was substituted with an alanine, and performed protein–lipid blot overlay assays using both transgenic parasites. The results showed lipid specificity of GlENTHp-HA for PI4P and $PI3,4,5P_3$ (Fig. 2A). On the other hand, the mutant $GlENTH_{K75A}$p-HA showed an ENTH domain defective in PIs binding, confirming that this residue is crucial for PIPs binding (Fig. 2A). By using the SNAP (screening for non-acceptable polymorphisms) method, which predicts the functional effects of single amino acid substitutions [36], we found that the mutation K75A was predicted as a non-neutral mutation, suggesting that the change of this specific amino acid can produce an alteration of the giardial ENTH function. To corroborate the lipid-plot assay, bile-stimulated *glenth-ha* and *glenthk75a* transgenic trophozoites were utilized for co-immunoprecipitation analysis using anti-$PI3,4,5P_3$ and anti-PI4P mAbs. It was shown that bile salts activate PI3K and the amount of available phosphoinositides in many cell types, including *Giardia* [47, 48, 53, 54; Gesumaria and Machado, personal communication]. The results showing that $PI3,4,5P_3$ and PI4P interacted with

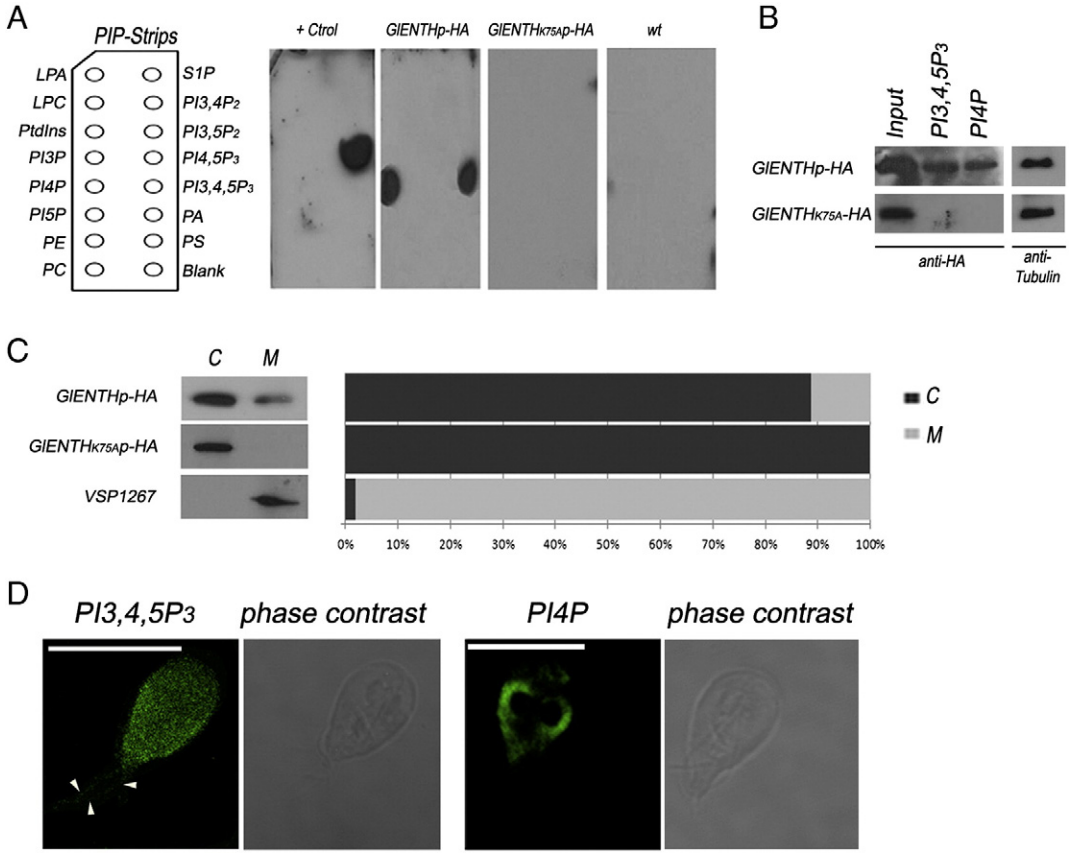

Fig. 2. GlENTHp binds to specific phosphoinositides. (A) GlENTHp interacts with $PI3,4,5P_3$ and PI4P. *glenth-ha*, *glenthk75a* and *wild-type* trophozoites were incubated with PIP-Strips and bound proteins detected with anti-HA mAb. + Ctrol: GST-tagged PLC-δ1 PH domain protein that binds to $PI4,5P_2$. Lysophosphatidic acid (LPA), lysophosphocholine (LPC), phosphatidylinositol (PtdIns), phosphatidylethanolamine (PE), phosphatidylcholine (PC), sphingosine 1-Phosphate (S1P), phosphatidic acid (PA), phosphatidylserine (PS). (B) Co-immunoprecipitation and immunoblot assays using anti-$PI3,4,5P_3$ or PI4P IgM mAbs and revealed with HRP-labeled anti-HA mAb, show that GlENTHp-HA, but not $GlENTH_{K75A}$-HA, interacts with these PIs. Input represents 5% of the total cells. These data show representative blots from one of two independent experiments. An aliquot of total cell lysate before immunoprecipitation for tubulin was used as a loading control. (C) *glenth-ha* and *glenthk75a* transgenic parasites were lysed under hypotonic conditions and the cytosolic (C) and membrane (M) fractions were recovered. The transmembrane protein VSP1267 was used as control. Densitometry data for each band for the relationship between C and M are given on the right. (D) Phosphoinositide localization in *Giardia* trophozoite. IFA and epifluorescence microscopy shows the cytoplasmic localization of $PI3,4,5P_3$ and PI4P in trophozoites. The presence of $PI3,4,5P_3$ in the flagella is denoted by arrowheads. Bars, 10 μM.

GlENTHp-HA but not with GlENTH$_{K75A}$p-HA, validate the lipid binding assay and verified that the K75 residue is necessary for lipid binding (Fig. 2B). Subcellular fractionation using hypotonic lysis of transgenic trophozoites indicated that GlENTHp-HA was primarily presented as cytosolic and at low levels as a membrane-bound population (Fig. 2C). Conversely, the mutated protein was present exclusively in the non-membrane fraction when cell fractionation was performed under hypotonic conditions (Fig. 2C), indicating that interaction between the ENTH domain and polyphosphoinositides was essential for membrane attachment of GlENTHp. As expected, the membrane protein VSP1267 used as control was restricted to the membrane fraction (Fig. 2C). Although many of the PIs are in low abundance in cells, a higher local concentration might be detected after stimulation by immunocytochemistry using anti-PIs antibodies [51, 55]. Thus, we decided to address the localization of PI3,4,5P$_3$ and PI4P in *Giardia* trophozoites using commercially available anti-PI3,4,5P$_3$ and anti-PI4P mAbs. While PI3,4,5P$_3$ was observed in the trophozoite body in punctate structures, enriched close to the plasma membrane (in the zone where the PVs are located) and also in the flagella (Fig. 2D, left panels), PI4P was localized in a pattern suggesting ER distribution with a clear enrichment around the nuclei (Fig. 2D, right panels).

3.3. GlENTHp interacts with AP-2, ubiquitin and participates in receptor-mediated endocytosis

To further analyze other associations of GlENTHp, we performed YTH analysis demonstrating that GlΔENTHp strongly interacted with αAP-2 but not with the μAP-2 subunit (Fig. 3A). Immunofluorescence and confocal microscopy showed that the cytoplasmic GlENTHp-HA colocalized with AP-2 in a region in close association with the PVs/

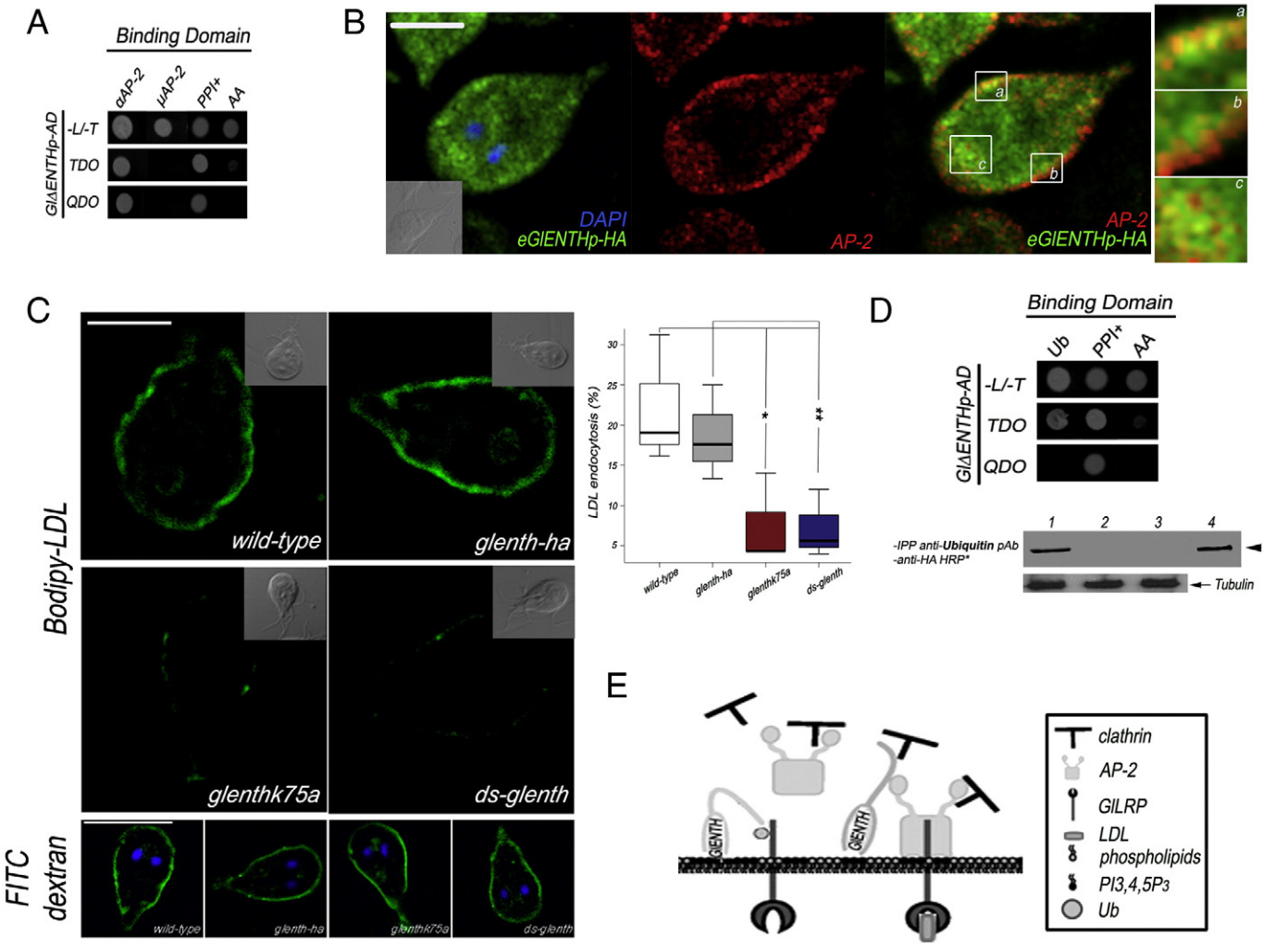

Fig. 3. GlENTHp participates in endocytosis. (A) The α subunit but not the medium subunits (μ) of AP-2 interacts with GlΔENTHp by YTH assay. To test protein interactions, the TDO and QDO selective mediums were used. (B) Direct IFA and confocal microscopy demonstrating that eGlENTHp-HA (green) and AP-2 (red) partially colocalize (eGlENTHp-HA/AP-2). Insets on the right magnify regions of the cell where the green and red fluorescence partially overlap (yellow). z-serie 9/31: 3.2 μm. Nuclei were stained with DAPI (blue). Differential interference contrast (DIC) microscopy is shown as insets. Bar, 5 μm. (C) Confocal fluorescence microscopy of Bodipy-LDL endocytosis (up to 30 min). FITC-dextran was used to test fluid-phase internalization. Nuclear DNA was labeled with DAPI (blue). Bar, 10 μm. Box-plot shows that Bodipy-LDL endocytosis decreases in *glenthk75a* and *ds-glenth* cells compared with *wild-type* trophozoites ($^*p < 0.05$, $^{**}p < 0.005$, respectively, by one-way ANOVA). Similar effects are observed when *glenth-ha,* and *ds-glenth* trophozoites are compared ($^{**}p < 0.005$). (D) Upper panel: The weak interaction between GlΔENTHp and Ubiquitin (Ub) is shown by cell growth in TDO but not in QDO selective medium. +PPI: Positive protein–protein interaction control. AA: Autoactivation negative control. Bottom panel: Co-immunoprecipitation experiment showing the association between GlΔENTHp and Ub. 1: GlENTHp-HA was immunoprecipitated from transgenic cells using an anti-Ub pAb. GlENTHp-HA (~50 kDa band, arrowhead) was detected by using HRP-labeled anti-HA mAb. 2: control using an irrelevant pAb. 3: control using untransfected cells. 4: Input lane. An aliquot of total cell lysate before immunoprecipitation for tubulin was used as a loading control. These data show representative blots from one of three independent experiments. (E) Proposed model for GlENTHp-driven endocytic internalization: GlENTHp proteins bind to PI3,4,5P$_3$ and the ubiquitinated receptor at the plasma membrane. GlENTHp in turn binds the endocytic proteins AP-2 and clathrin. Through a specific internalization motif present in its cytoplasmic tail, the LDL receptor, GILRP, binds the AP-2 complex. Adapted from [72].

plasma membrane in cells expressing GlENTHp-HA under its endogenous promoter (Fig. 3B). Colocalization analysis of stacked slides showed that both proteins partially colocalized, showing a Manders' overlap coefficient (M) of 0.754. This colocalization was most notorious in *glenth-ha* transgenic cells (M of 0.882) (Fig. S4A). One approach to address the specific role of GlENTHp was to perform functional analysis using transgenic cells overexpressing either GlENTHp-HA, the mutant GlENTH$_{K75A}$p-HA or trophozoites that produce double-stranded RNA from the **p**ds-glenth vector in a Tet-inducible fashion (Fig. S1B) [49]. Real-time PCR (qRT-PCR) showed an increase in the mRNA expression in *glenth-ha* and *glenthk75a* cells, and a significant reduction in the expression of native *glenth* mRNA in *ds-glenth* (transgenic trophozoites deficient in *glenth* mRNA) compared with *wild-type* trophozoites (Fig. S5). Therefore, we used the *glenth-ha*, *glenthk75a*, and *ds-glenth* transgenic cells to address the role of GlENTHp in receptor-mediated endocytosis by adding the fluorescent low density lipoprotein (Bodipy-LDL) to the culture medium and testing the endocytosis in living trophozoites, as we performed previously [7]. Images showed a major decrease of LDL internalization in *glenthk75a* and *ds-glenth* trophozoites compared with *wild-type* and *glenth-ha* cells (Fig. 3C, Bodipy-LDL). When fluid-phase endocytosis using FITC-dextran was tested, no difference was observed between these cells in the internalization of these inert molecules (Fig. 3C, FITC-dextran) [7]. Immunofluorescence-based quantitation of Bodipy-LDL clearly showed that there is a significant reduction in LDL endocytosis in *glenthk75a* and *ds-glenth* cells, showing the active participation of GlENTHp in LDL receptor-mediated endocytosis (Fig. 3C, box-plot) and supporting the hypothesis of GlENTHp acting as an adaptor for endocytosis.

Epsins from different species also contain one or more ubiquitin-interacting motifs (UIMs) that interact with ubiquitinated cargo [56, 20, 57, 22]. However, the GlENTHp C-terminal domain does not present UIMs or canonical motifs for interacting with clathrin and clathrin adaptors. Because the interaction of many members of the epsin family with a variety of binding partners at their C-terminus has been revealed in the absence of conserved domains, we decided to analyze the interaction of GlΔENTHp with ubiquitin. YTH analysis showed that the C-terminus of GlENTHp interacted weakly with ubiquitin (Ub) (Fig. 3D, top panels). However, co-immunoprecipitation assays confirmed the interaction between GlENTHp and Ub (Fig. 3D, bottom panel). The results prompted us to propose a model for LDL receptor-mediated endocytosis in which GlENTHp proteins bind to PI3,4,5P$_3$ and the ubiquitinated receptor at the plasma membrane. Sequentially, GlENTHp binds αAP-2 and clathrin. The LDL receptor, GlLRP, will also bind μAP-2 through the endocytic motif present in the receptor cytoplasmic domain (Fig. 3E).

3.4. GlENTHp also participates in the lysosomal-protein trafficking via AP-1

While epsin1–3 colocalizes with AP-2 and clathrin, epsinR was shown to be associated with AP-1 and GGAs as well as clathrin in the Golgi membranes [24]. When we performed YTH analysis to test the interaction with AP-1, the results showed that GlΔENTHp strongly interacted with γAP-1but no association was observed when the μAP-1 subunit was assessed (Fig. 4A). As mentioned, a typical Golgi complex with organized and parallel cisternae is not apparent in vegetative *Giardia* trophozoites and it was suggested that specific domains of the ER (called ER-exit sites) might play a critical role in protein sorting to different subcellular compartments [4]. To investigate whether GlENTHp localized to these particular sorting regions, we tested the colocalization of GlENTHp-HA and the ER-chaperone BiP, since it was demonstrated that BiP and the COPII coatomer subunit Sec23 colocalized at the ER-exit sites [58]. We observed that GlENTHp and BiP proteins partially overlapped in distinct ER-spots (Fig. 4B), with this observation being supported by the results of the coefficient calculations of 0.655 for M. Moreover, this colocalization was enhances in *glenth-ha* transgenic cells (M of 0.863) (Fig. S4B).

Because AcPh is transported from the ER to the PVs via its receptor, GlVps, and AP-1 [6], we decided to assess the role of GlENTHp in ER-to-PV trafficking by analyzing the activation of the hydrolase AcPh at the PVs. The results showed a defect in AcPh activity only in *glenthk75a* and *ds-glenth* transgenic trophozoites (Fig. 4C, ELF97), with a pattern of mislocalization coincident with the downregulation of the GlVps [6]. Addition of LysoTracker to these cells showed no alteration in the pH of PVs, undermining the possibility of a loss of AcPh activity by alteration of the PV environment (Fig. 4C, LysoTracker). Analysis of the fluorescent area showed significant reduction in AcPh activation of *glenthk75a* and *ds-glenth* transgenic trophozoites relative to *wild-type* or *glenth-ha* cells (Fig. 4C, box-plot). These new results prompted as to proposed an additional model in which the ENTH domain of GlENTHp binds to PI4P present at the ER-exit site membrane while its C-terminal region is able to recruit GlVps (associated with AcPh), AP-1 and clathrin, leading to protein segregation and membrane deformation (Fig. 4D).

3.5. Differential expression of GlENTHp alters vacuolar homeostasis

PVs have been described as oval-shaped vacuoles, heterogeneous in size and density [9, 59]. When the fine structure of trophozoites was assessed, we observed that *wild-type* cells conserved the electron-dense heterogeneity of the PVs but *glenth-ha* cells showed homogeneous electron-lucent PVs (Fig. 5A–B). Conversely, *glenthk75a* and *ds-glenth* transgenic cells caused accumulation of electron-dense material in the PVs compared with *wild-type* trophozoites (Fig. 5A–B). True differences were only observed between *ds-glenth* cells and the rest of the groups (One-Way ANOVA, $p < 0.01$ and Tukey's test). Also, no significant differences were found between *glenth-ha* transgenic trophozoites and *wild-type* cells using a paired difference test (Welch's *t*-test). Interestingly, the PVs observed in *glenthk75a* cells were larger than the PVs from wild-types (Fig. 5C), resembling the finding of enlarged PVs in cells expressing the mutant of giardial dynamin (DRP-mut) [60]. Our findings suggest that GlENTHp also participates in the trafficking of material in and out of the PVs during *Giardia* growth, emphasizing the multifaceted characteristic of these organelles, which may also act as sorting stations.

3.6. The function of GlENTHp is critical for Giardia growth

Like *ds-glenth* or *glenthk75a* cells, trophozoites treated with the microbicidal lactoferrin (LF) or the N-terminal antimicrobial peptides (LFpep) showed accumulation of electron-dense material in the PVs [61] and drastically affected trophozoite growth [62]. This prompted us to perform growth curves in order to analyze whether there might be any alteration in *glenth-ha*, *glenthk75a* or *ds-glenth* cell growth. Because downregulation of GlENTHp required the induction of *glenth* dsRNA by tetracycline (Tet) addition, a control adding the same amount of drug to *wild-type* cells was tested. Addition of Tet to *wild-type* cells resulted in a non-significant decrease in cell growth compared with cell cultures without tetracycline (Fig. 6). We observed that *ds-glenth* and *glenthk75a* transgenic cells caused a severe growth defect (Fig. 6), which correlated with the PV becoming more electron-dense. Conversely, no significant effect in cell growth was observed in *glenth-ha* cells (Fig. 6). These results indicated an association between cell growth and accumulation of dense material in the PVs.

3.7. GlENTHp shuttling between the cytoplasm and the nuclei relies on its binding to PIs

Direct immunofluorescence analysis and confocal microscopy showed an increased localization of GlENTH$_{K75A}$p-HA in one of the nuclei in transgenic parasites compared with GlENTH-HA (Fig. 7A). These results raise the possibility that the retention of GlENTHp in the nucleus depends on its ability to bind PIs. LY294002, but not

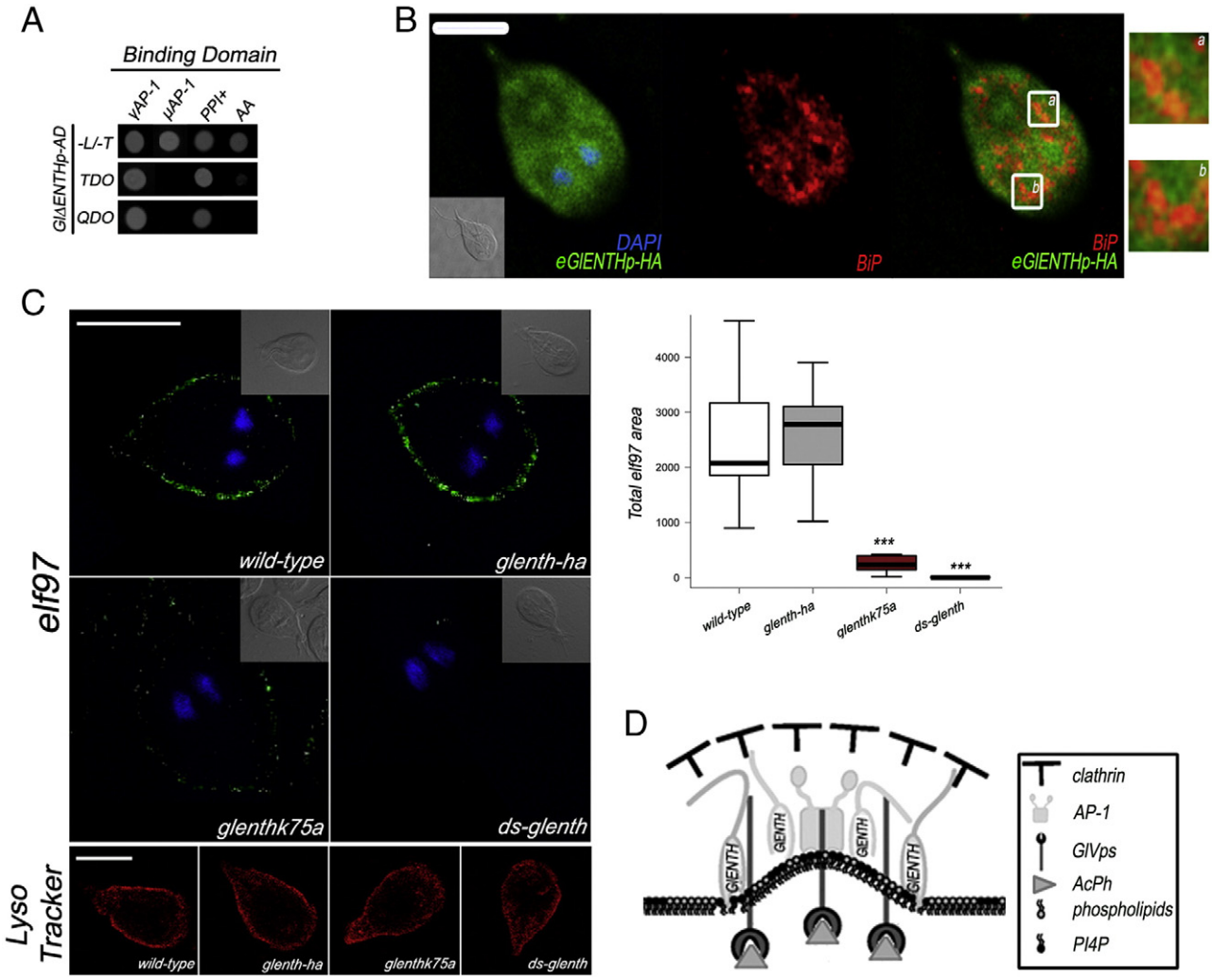

Fig. 4. GlENTHp participates in the trafficking of soluble hydrolases to the PVs via AP-1. (A) The γAP-1 but not the μAP-1 subunit interacts with GlΔENTHp by YTH assay. To test protein interactions the TDO and QDO selective mediums were used. (B) Direct IFA and confocal microscopy show that eGlENTHp-HA (green) partially colocalizes with the ER-resident chaperone BiP (red) in the ER (eGlENTHp-HA/BiP). Insets on the right magnify regions of the cell where the green and red fluorescence partially overlap (yellow). z-serie 7/31: 1.2 μm. Nuclei were stained with DAPI (blue). Differential interference contrast (DIC) microscopy is shown as insets. Bar, 5 μm. (C) By using the ELF97 at pH 5.5, a notable reduction of acid phosphatase activity is observed in *glenthk75a* and *ds-glenth* compared with *wild-type* and *glenth-ha* trophozoites. Nuclear DNA was labeled with DAPI (blue). PV acidification is preserved in all cells as shown by the consistent fluorescence of LysoTracker. Bar, 10 μm. The box-plot shows the quantitative fluorescent measurements of ELF97 (acid phosphatase activity). A significant decrease in mean fluorescence in *glenthk75a* and *ds-glenth* cells is observed when compared with *wild-type* and *glenth-ha* cells (***$p < 0.0001$, one-way ANOVA). (D) Proposed model for GlENTHp clathrin assembly at the ER in *Giardia*. The ENTH domain of GlENTHp binds to PI4P leading to membrane deformation and curvature. GlENTHp may also recruit the acid phosphatase receptor GlVPS, AP-1 and clathrin to nascent vesicles through its C-terminal region. Adapted from [72].

Wortmannin, was shown to impair trophozoite growth at 5 to 250 μM and affect the role played by the PI3 kinase in the *G. lamblia* cell cycle [50, 63]. When these transgenic cells were treated with LY294002 to reduce PI3,4,5P_3 and PI4P synthesis, a significant increase was observed in nuclear localization of GlENTHp-HA of cells treated with LY294002 (GlENTHp-HA+) compared with GlENTHp-HA without the inhibitor (Fig. 7A–B). In contrast, the presence of GlENTH$_{K75A}$p-HA inside a nucleus remained unchanged in transgenic *glenthk75a* cultures with (GlENTH$_{K75A}$p-HA+) or without LY294002 treatment (Fig. 7A–B). Clearer results were observed when GlENTHp nuclear localization was statistically analyzed in these cells (Fig. 7, box-plot), suggesting that this protein may continuously shuttle in and out of the nuclear envelope, depending on the ability of the PIs to retain GlENTHp outside the nucleus and associated to membranes, as was observed for other ENTH domain-containing proteins [64]. Remarkably, GlENTHp-HA- and GlENTH$_{K75A}$p-HA-enhanced nuclear localization did not occur in both nuclei equally, but frequently only one nucleus was found to be positive (see discussion).

4. Discussion

A key mechanism for establishing and maintaining subcellular compartmentalization is the formation of membrane-bound transport vesicles that assemble at the cytosolic surface of a donor compartment to deliver specific cargo molecules to an appropriate acceptor compartment. Clathrin-coated vesicles are the best-characterized type of transport vesicles, mediating cargo delivery to endosomal/lysosomal compartments in all eukaryotic cells. The endosomal/lysosomal system in *Giardia* exhibits significant complexity and diversity in terms of morphology and function, but its transport machinery is fairly well conserved [5]. We previously suggested that this organism preserved a highly reduced set of proteins involved in endosomal/lysosomal trafficking, with the participation of two of the four AP complexes, AP-1 and AP-2 but no monomeric adaptor proteins. In this study, we characterize the protein GlENTHp, which contains a conserved N-terminal ENTH domain characteristic of the ENTH/ANTH/VHS superfamily of monomeric adaptor proteins involved in endosomal–lysosomal protein

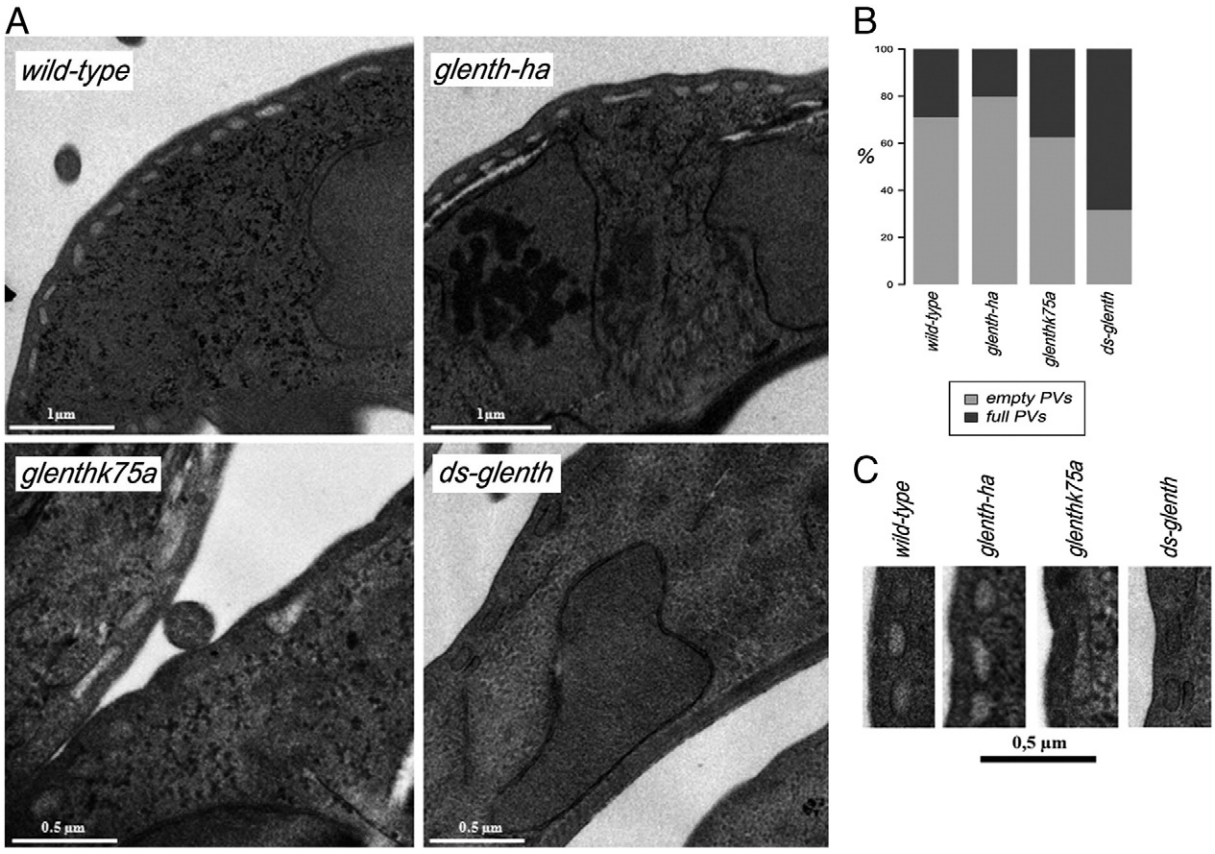

Fig. 5. GlENTHp dysfunction affects PV homeostasis. (A) Electron micrographs showing altered electron opacity of PVs in transgenic trophozoites. Transmission electron microscopy (TEM) of trophozoites shows that the interiors of individual PVs vary in electron opacity, suggesting vacuoles of differing content (*wild-type*). Cells overexpressing GlENTHp-HA (*glenth-ha*) show a loss of electron-dense material in most of the PVs analyzed. Conversely, *glenthk75a* and *ds-glenth* transgenic trophozoites show accumulation of electron-dense material in all PVs. Scale bars: 0.5 µm. Images are representative of three independent experiments with n = 20 cells. (B) The graphic shows quantitative analysis of the relationship between PVs containing electron dense material (full PVs) and PVs containing electron lucent material (empty PVs). *glenthk75a* and *ds-glenth* cells showed a numerical increase of full PVs when compared to *wild-type* and *glenth-ha* cells. (C) Comparative TEM shows in detail enlarged PV in *glenthk75a* and electron dense material in PVs of *glenthk75a* and *ds-glenth* transgenic cells. Images are to scale.

trafficking, from Golgi to endosomes, between endosomes, and in the endocytic process [65, 66]. The findings presented here suggest that GlENTHp is also involved in clathrin-mediated trafficking in this parasite, questioning the original idea of the exclusive role of heterotetrameric adaptor proteins in this pathway.

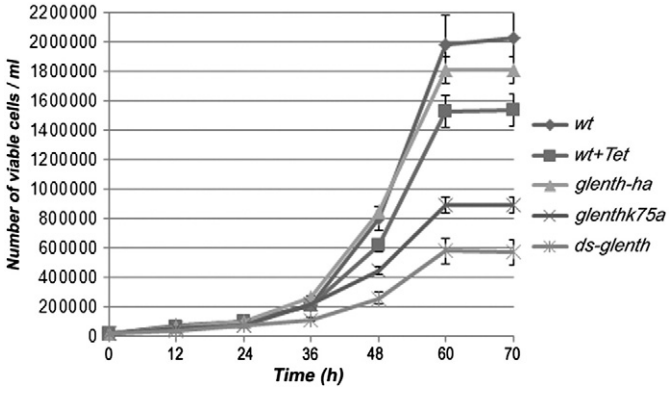

Fig. 6. GlENTHp plays a critical role in *Giardia* growth. *Wild-type*, *glenth-ha*, *glenthk75a*, and *ds-glenth* growth curves: at time 0, 1.8×10^4 trophozoites were inoculated to growth medium and trophozoite numbers were determined every 12 h. Tet addition to *wild-type* (*wt* + Tet) showed a minor effect on growth compared to cultures without Tet. The growth of *ds-glenth* trophozoites is dramatically reduced compared with *wild-type* and *wt* + Tet cells. A significant reduction in growth is also observed in *glenthk75a* but not in *glenth-ha* compared with *wild-type* cells. Data represent the mean ± s.d. for n = 10 in three independent experiments.

Both epsin and epsinR contain the ENTH domain and play fundamental roles in clathrin-mediated endocytosis at the plasma membrane and in clathrin-mediated budding from the trans-Golgi network to the endosomes, respectively [66]. Recent results support the hypothesis that the ENTH domain from epsinR is the foundation of the superfamily, as it is present in different eukaryotic organisms from *H. sapiens* to *G. lamblia* [27], with this domain being the only representative of the ENTH/ANTH/VHS function in Chromista (e.g. *T. gondii*), Euglenosoa (e.g. *T. brucei*) and Excavata (e.g. *G. lamblia*) taxa, thus suggesting that multiple tasks may be performed by the unique epsinR-like proteins. In agreement with this hypothesis, we found that GlENTHp contains the characteristic of both epsin and epsinR monomeric adaptors, although a dissection of the role of its interacting partners are required to define GlENTHp as an epsin-like protein.

The ENTH domain plays an important role in the creation of membrane curvature by binding specific PIs enriched in certain patches of the membranes [19, 67]. The ENTH domain of epsin1 has been shown to bind to $PI4,5P_2$ [18], while epsinR binds preferentially to PI4P with a less strong interaction with PI5P; $PI3,4P_2$ and a minor binding to $PI3,5P_2$ and $PI3,4,5P_3$ [25]. In this work, we showed that GlENTHp bonded to $PI3,4,5P_3$ and PI4P, with the K75 residue of the ENTH domain being critical for these interactions as was observed previously in COS-7 and *Dictyostelium* cells [18, 52]. Although PIs have not been well-described in *Giardia*, three phosphatidylinositol kinases (PIK) and phosphatidylinositol phosphatase are present in the *Giardia* genome, and recent results showed that the PIK genes are expressed during the entire cell cycle [68]. It was suggested that synthesized PIs can be utilized to generate PI3P; PI4P; $PI4,5P_2$ and $PI3,4,5P_3$ by giardial PIKs for cellular

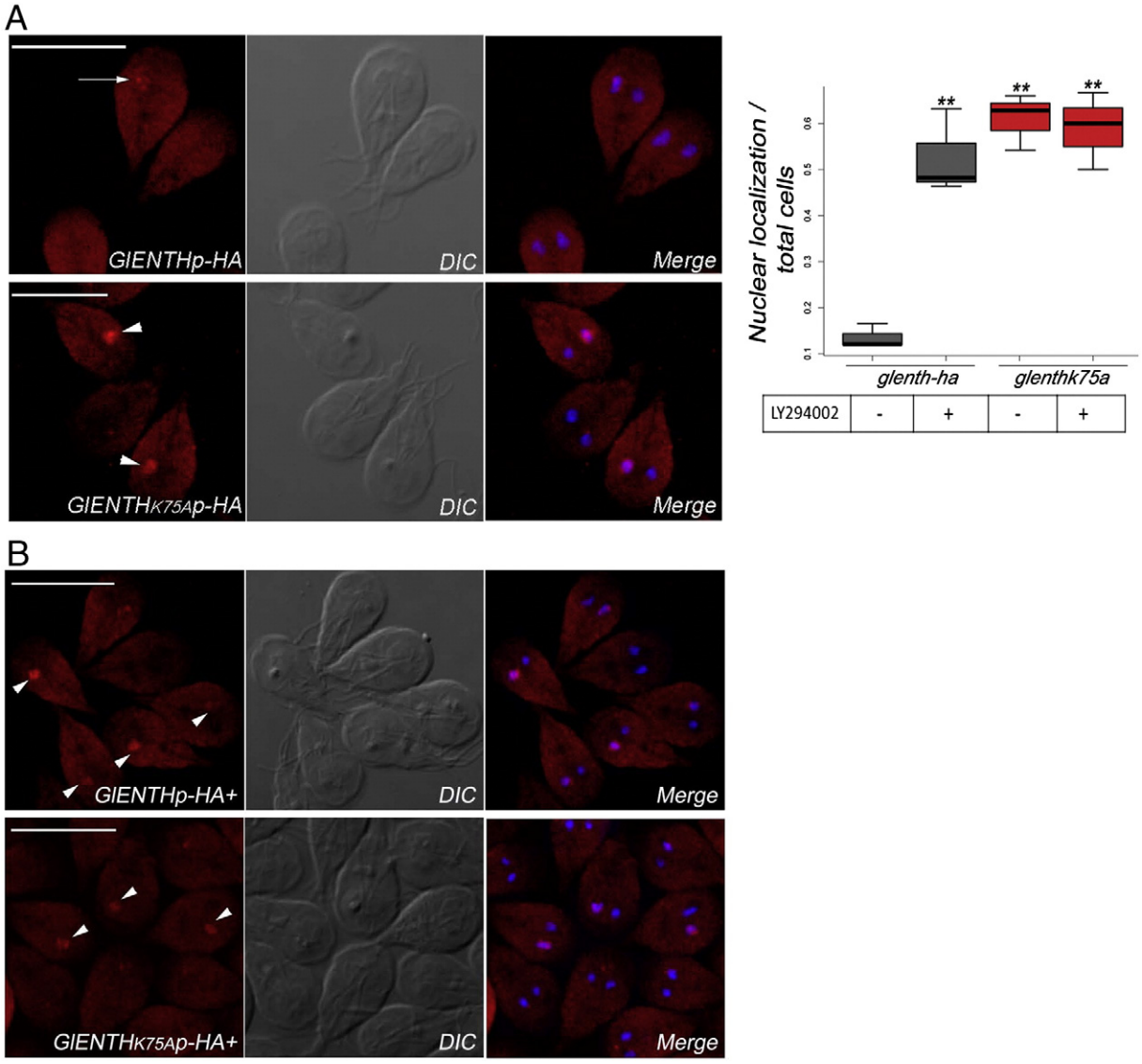

Fig. 7. GlENTHp shuttles between the cytoplasm and the nuclei. (A) IFA and confocal microscopy shows GlENTHp-HA and GlENTH$_{K75A}$p-HA in the cytoplasm and inside one nucleus (arrow and arrowheads) of transgenic parasites. Note the high accumulation of GlENTH$_{K75A}$p-HA in one of the nuclei (arrowhead). Nuclei were stained with DAPI. DIC: Differential interference contrast microscopy. Bar, 10 μM. (B) IFA and confocal microscopy shows that GlENTHp-HA nuclear localization is significantly greater when 30 μM of LY294002 was added to the culture medium for 24 h (GlENTHp-HA+). No significant changes in nuclear localization are observed for GlENTH$_{K75A}$p-HA in treated healthy cells (GlENTH$_{K75A}$p-HA+). Nuclei were stained with DAPI. DIC: Differential interference contrast microscopy. Bar, 10 μM. Box-plots shows the ratio of cells with nuclear localization of HA-tagged protein to total cells in *glenthp-ha* and *glenthk75a* untreated and treated (+) cells. At least 1000 trophozoites were assessed three times per condition. Accumulation of GlENTHp+, GlENTH$_{K75A}$p-HA and GlENTH$_{K75A}$p-HA+ in the nuclei is consistent and significant (**$p < 0.0001$ by Student's *t*-test).

signaling [50, 68], but it was not demonstrated until recently that *Giardia* is able to produce PI3P, PI4P and PI4,5P$_2$ [69; Gesumaria and Machado, personal communication]. Supporting these new findings, we detected PI4P in an ER pattern and concentrated around the nuclei in trophozoites, suggesting that this might be the lipid that binds GlENTHp to the sorting station or ER-exit sites. Regarding PI3,4,5P$_3$, we found that this PI is expressed at low levels in intracellular punctate structures in the cytoplasm and enriched close to the plasma membrane. PI3,4,5P$_3$ exists as a persistent pool in the cytosol, plasma membrane and phagosome of *E. histolytica* and a nonpathogenic amoeba, *D. discoideum*, suggesting that it may be required for the continuous uptake of nutrients in these lower eukaryotes, a common characteristic of protozoa including *Giardia* [70, 71].

While the N-termini of ENTH/ANTH/VHS proteins are well conserved, the C-terminal parts are highly divergent, frequently specific to each family or subfamily, and recruit clathrin coat components, driving the clathrin-assembly and sorting of cargo [72, 73]. In this work, we experimentally verified that GlENTHp binds to clathrin, αAP-2, γAP-1 and Ub. However, neither typical DPW (Asp-Pro-Trp) motifs, essential for AP-2 binding, nor clathrin boxes (LLDLD/LIELE), involved in clathrin binding, are present in its primary structure. Similar to GlENTHp, no LLDLD/LIELE clathrin boxes are part of the epsinR sequence from *T. brucei* (TbEpsinR), but it was proved that it associates in a complex with clathrin, and that this association is required for TbEpsinR targeting to membranes [26]. Nevertheless, since the original definition of the clathrin box motif, several variant clathrin box motifs and non-canonical-binding motifs have been identified [74]. Like epsinR, no NPF (Asn-Pro-Phe) repeats that are required for binding EH domain-bearing proteins, such as Eps15, have been observed, suggesting that GlENTHp is more distantly related to epsins 1–3. Although proved by experimental analysis, the presence of the DFxDF binding motifs for AP1/GGA is not found in GlENTHp. The lack of these motifs is consistent with the absence of GGAs homologous protein in the *Giardia* genome. Unlike what was shown in other organisms in which epsins directly interact with the clathrin at the N-terminal β-propeller domain [75, 76], GlENTHp binds to a giardial clathrin sequence adjacent to the

C-terminus. It was suggested that the juxtaposition of multiple clathrin-binding sites might increase the affinity for a soluble clathrin trimer, improving the efficiency of clathrin coat polymerization at bud sites on the cell surface [75, 77]. Unusually, neither typical membrane-associated clathrin lattices nor emerging clathrin-coated pits have been observed in this parasite. Instead, uncharacteristic coated pits were seen in close association with the PVs [11], suggesting that a distinct arrangement of clathrin that differs from the formation of clathrin trimer and cages might occur in this parasite [78]. It is thus possible that the giardial clathrin-specific interaction with GlENTHp (and other adaptor proteins) defines a particular complex array forming atypical structures. The interaction of GlENTHp with clathrin, α2 and γ1 disclosed that the occurrence of sequence motifs together with the conservation of short linear binding motifs is highly divergent in this early branching eukaryote cell. No putative UIMs were detected in GlENTHp. Moreover, because no shift in the molecular mass of the ~50 kDa band of GlENTHp was observed in immunoblotting nor was GlENTHp identified as an ubiquitinated protein in the in vitro ubiquitination screening [79], it is most likely that GlENTHp binds ubiquitinated receptors. The interaction of GlENTHp with ubiquitin shown in this work suggests that recruitment of ubiquitin to the ENTH-domain proteins is not a specific innovation restricted to higher eukaryotes [26]. Remain to be analyzed whether GlENTHp is able to bind more than one Ub molecule. It was reported that epsinR from humans (syn. CLINT) contains a carboxyl-terminal methionine-rich domain (Met427-Met605), which contains more than 17% methionine at its C-terminus [80]. The presence of this domain has not been extensively corroborated but analysis of the amino acid composition of GlENTHp showed that it in fact possesses a segment Met_{191} to Met_{403} that contains 32 methionine residues (15%), 22 of which are clustered in the segment Met_{241}–Met_{354} (22%). Comparison of this segment with the ones corresponding to the human Epsin and EpsinR showed that GlENTHp may possess a carboxyl segment enriched in methionine residues (Zamponi and Touz, unpublished results). The GlENTHp C-terminus is also enriched in proline (P) and glutamine (Q) residues, similar to the epsinR-like from *T. brucei*, a *Giardia* close related organism, which showed no clathrin binding domains but binds to clathrin heavy chain [26].

A major obstacle in identifying which particular pathway is utilized by *Giardia* for cell growth and differentiation is the limited set of specific ligands and organelle-subdomain markers present in this parasite. Because *Giardia* lacks endosomes and Golgi apparatus, the lysosome-like PVs and the ER act as an endosomal-lysosomal compartment and sorting station, respectively. In this regard, we observed that GlENTHp is mainly cytosolic, very close to the plasma membrane partially colocalizing with AP-2 and also in close association with the ER-chaperone BiP, respectively. Recently, we found that LDL is endocytosed for nutritional purposes via an LDL-receptor-related protein and AP-2 [12], while AcPh is transported from the ER to the PVs by its GlVps receptor coupled to AP-1 [6]. Thus, both LDL and AcPh proved to be attractive candidates to be specifically tracked down using a knock-down strategy. We found that, when GlENTHp was downregulated, LDL internalization was suppressed or significantly reduced. The same effect was observed in the *glenthk75a* trophozoites, suggesting that the interaction of GlENTHp with the membranes is critical to accomplishing LDL receptor-mediated endocytosis. On the other hand, the alteration of AcPh activity in these two transgenic cells might be directly linked to the ability of GlENTHp to support ER-to-PV trafficking. Due to its unusual characteristics and the functional results we presented here, we propose that GlENTHp may play a dual function depending on the trophozoite requirement for endocytosis (e.g. for nutrition purpose, for remodeling the plasma membrane composition or for regulation of signaling) or for lysosomal protein sorting (e.g. for digestion purposes).

We showed here that either downregulation of GlENTHp or overexpression of a nonfunctional GlENTHp resulted in a remarkable decrease in trophozoite growth and an unusual accumulation of dense material in the PVs. These characteristics were observed by treating *wild-type* trophozoites with LF (or LFpep), a natural antimicrobial metabolite and one of the most important host defenses against *Giardia* [62, 81]. Although LF's microbicidal action was originally attributed to its ability to sequestrate iron from susceptible organisms, LF causes more rapid killing than iron deprivation, and the killing is not prevented by iron [61]. Moreover, it was shown that LF and LFpep bind to trophozoites and induce significant ultrastructural damage and accumulation of electron-dense material in the PVs [61, 62]. A similar effect was observed after addition of LY294002, which showed a marked giardicidal effect and a complete disorganization of the array of the PVs [63]. It has been demonstrated in other cells that LF is internalized by lactoferrin receptor via clathrin-mediated endocytosis [82] and that LF specifically inhibits endocytosis of chylomicron [83], but more information is necessary to understand whether there is a correlation between LF, LDL/chylomicron endocytosis, PIs and GlENTHp in *Giardia*. Our ongoing results suggest that there is a correlation between GlENTHp expression (and other molecules involved in adaptin-clathrin endocytosis), LF internalization and cell growth. Also, the accumulation of dense material in the PVs, together with a noticeable enlargement of the vacuoles in *glenthk75a* cells, suggests that GlENTHp may possess an additional role in sorting and vesicle budding from the PVs in conjunction with giardial dynamin, clathrin, and AP-2 [7, 60]. Thus, the formation of larger PVs could be caused by a failure in the budding or fission of AP-2/clathrin coated vesicles when mutated GlENTHp or dynamin, respectively, act as negative mutants. Although it was suggested that the cargo dynamics of PVs involved vertical exchange (from plasma membrane to PVs to ER/nuclear envelope), our recent results showed that it is possible that GlENTHp is also involved in lateral vesicular PV-to-PV movement for PV maturation [6].

When the localization of the mutant $GlENTH_{K75A}$-HA was analyzed, we observed that it was significantly accumulated inside one of the nuclei, like the epsin1-mutant K76A in COS-7 cells [18]. Moreover, after addition of the PI3-kinase inhibitor LY294002, the localization of GlENTHp-HA in one of the nuclei dramatically increases. Possibly, this inability to recognize the PIs prevents its retention in the membrane pool then showing greater presence in the nuclei. These results point to a general cytoplasmic but also nuclear distribution of GlENTHp, supporting the observation that this protein may also play a role in a signaling pathway linking the endocytic machinery to the regulation of nuclear function [64]. Also, PI3-kinase signaling plays a role in cell proliferation and survival [84] and, therefore, the presence of $PI3,4,5P_3$ in *E. histolytica*, *D. discoideum* and *G. lamblia* may also be related to their single-cell nature, for which rapid and continuous divisions are an important goal [70]. However, whether the interaction between the ENTH domain of GlENTHp and $PI3,4,5P_3$ is essential for signaling remains to be elucidated. It was shown that each giardial nucleus presents exceptionally different pore complex number, distribution, and clustering [85], which might explain the presence of GlENTHp or the accumulation of $GlENTH_{K75A}$-HA in one of the nuclei. Although it was demonstrated that the extensive direct passageway across the nuclear envelope occurs through nuclear pore complexes [86], the function of the nuclear envelope in *Giardia* has been poorly studied. Also, differences in chromosome number between the two nuclei seem to occur in certain *Giardia* isolates [87] and the expression of the small nucleolar RNA GlsR17 was found to occur primarily in only one nucleolus [88]. These observations suggest that the asymmetry of both nuclei gives *Giardia* spp. unique possibilities for the regulation of gene expression, as could be the case for the regulation of GlENTHp. In any case, although we cannot completely exclude a general nuclear protein sorting in which one nucleus is more active than the other, certainly, the localization of GlENTHp in one of the nuclei is a particularity of this protein.

During the review process of this manuscript, a Short Communication by Ebneter & Hehl was published showing that GlENTHp (named GlEpsin in this communication) mainly localized in the giardial ventral disk [89]. It is possible that the misslocalization of Glepsin is due to a fixation artifact. Considering that the immunofluorescence assay was not

described in the communication, it is hard to evaluate whether this was the case. Also, Ebneter & Hehl showed that Glepsin N-terminal domain produced in *E. coli* binds only to PI3,4,5P_3, probably because the expression of Glepsin N-terminal domain in bacteria might not behaves exactly as the whole protein expressed in *Giardia*. Finally, Ebneter & Hehl specified that Glepsin (GlENTHp) do not bind to any endosomal components, including clathrin. However, no results supported this statement.

The multifunctional role of GlENTHp is consistent with the evidence that *Giardia* possesses many proteins with combined functions and can be considered as having a minimalist version of the more complex trafficking machinery present in other eukaryotes. Further analysis of GlENTHp, by combining biochemical, pharmacological, genetic and cell-biological approaches, will yield new insights into the function of PVs and may provide new avenues for therapeutic intervention against *Giardia* and related parasites.

Transparency document

The Transparency document associated with this article can be found, in the online version.

Supplementary data to this article can be found online at http://dx.doi.org/10.1016/j.bbamcr.2014.12.034.

Acknowledgements

This research was supported by the Argentine Agencia Nacional para la Promoción de la Ciencia y Tecnología (FONCyT-PICT2010-737). The authors would like to thank María R. Rivero, Cecilia V. Vranych, María C. Merino and Silvana L. Miras for their insightful suggestions and comments, and Carla Cisternas and Florencia Daddan for help with the qRT-PCT assay. We thank Dr. Celeste Gesumaría and Dr. Estela Machado for sharing their results on the presence of PIs in *Giardia*.

References

[1] S. Munro, Organelle identity and the organization of membrane traffic, Nat. Cell Biol. 6 (2004) 469–472.
[2] E. Perret, A. Lakkaraju, S. Deborde, R. Schreiner, E. Rodriguez-Boulan, Evolving endosomes: how many varieties and why? Curr. Opin. Cell Biol. 17 (2005) 423–434.
[3] E. van Meel, J. Klumperman, Imaging and imagination: understanding the endo-lysosomal system, Histochem. Cell Biol. 129 (2008) 253–266.
[4] C. Faso, A.B. Hehl, Membrane trafficking and organelle biogenesis in *Giardia lamblia*: use it or lose it, Int. J. Parasitol. 41 (5) (2011) 471–480. http://dx.doi.org/10.1016/j.ijpara.2010.12.014.
[5] M.C. Touz, M.R. Rivero, S.L. Miras, J.S. Bonifacino, Lysosomal protein trafficking in *Giardia lamblia*: common and distinct features, Front. Biosci. (Elite Ed.) 4 (2012) 1898–1909.
[6] M.R. Rivero, S.L. Miras, C. Feliziani, N. Zamponi, R. Quiroga, S.F. Hayes, A.S. Ropolo, M.C. Touz, Vacuolar protein sorting receptor in *Giardia lamblia*, PLoS ONE 7 (2012) e43712.
[7] M.R. Rivero, C.V. Vranych, M. Bisbal, B.A. Maletto, A.S. Ropolo, M.C. Touz, Adaptor protein 2 regulates receptor-mediated endocytosis and cyst formation in *Giardia lamblia*, Biochem. J. 428 (2010) 33–45.
[8] S.A. House, D.J. Richter, J.K. Pham, S.C. Dawson, Giardia flagellar motility is not directly required to maintain attachment to surfaces, PLoS Pathog. 7 (2011) e1002167.
[9] D.E. Feely, J.K. Dyer, Localization of acid phosphatase activity in *Giardia lamblia* and *Giardia muris* trophozoites, J. Protozool. 34 (1987) 80–83.
[10] D.G. Lindmark, *Giardia lamblia*: localization of hydrolase activities in lysosome-like organelles of trophozoites, Exp. Parasitol. 65 (1988) 141–147.
[11] A. Lanfredi-Rangel, M. Attias, T.M. de Carvalho, W.M. Kattenbach, W. De Souza, The peripheral vesicles of trophozoites of the primitive protozoan *Giardia lamblia* may correspond to early and late endosomes and to lysosomes, J. Struct. Biol. 123 (1998) 225–235.
[12] M.R. Rivero, S.L. Miras, R. Quiroga, A.S. Ropolo, M.C. Touz, *Giardia lamblia* low-density lipoprotein receptor-related protein is involved in selective lipoprotein endocytosis and parasite replication, Mol. Microbiol. 79 (2011) 1204–1219.
[13] M.R. Rivero, I. Jausoro, M. Bisbal, C. Feliziani, A. Lanfredi-Rangel, M.C. Touz, Receptor-mediated endocytosis and trafficking between endosomal–lysosomal vacuoles in *Giardia lamblia*, Parasitol. Res. 112 (2013) 1813–1818.
[14] M.C. Touz, L. Kulakova, T.E. Nash, Adaptor protein complex 1 mediates the transport of lysosomal proteins from a Golgi-like organelle to peripheral vacuoles in the primitive eukaryote *Giardia lamblia*, Mol. Biol. Cell 15 (2004) 3053–3060.
[15] A.G. McArthur, H.G. Morrison, J.E. Nixon, N.Q. Passamaneck, U. Kim, G. Hinkle, M.K. Crocker, M.E. Holder, R. Farr, C.I. Reich, G.E. Olsen, S.B. Aley, R.D. Adam, F.D. Gillin, M.L. Sogin, The Giardia genome project database, FEMS Microbiol. Lett. 189 (2000) 271–273.
[16] J.S. Bonifacino, L.M. Traub, Signals for sorting of transmembrane proteins to endosomes and lysosomes, Annu. Rev. Biochem. 72 (2003) 395–447.
[17] L. Maldonado-Baez, B. Wendland, Endocytic adaptors: recruiters, coordinators and regulators, Trends Cell Biol. 16 (2006) 505–513.
[18] T. Itoh, S. Koshiba, T. Kigawa, A. Kikuchi, S. Yokoyama, T. Takenawa, Role of the ENTH domain in phosphatidylinositol-4,5-bisphosphate binding and endocytosis, Science 291 (2001) 1047–1051.
[19] M.G. Ford, I.G. Mills, B.J. Peter, Y. Vallis, G.J. Praefcke, P.R. Evans, H.T. McMahon, Curvature of clathrin-coated pits driven by epsin, Nature 419 (2002) 361–366.
[20] S. Polo, S. Sigismund, M. Faretta, M. Guidi, M.R. Capua, G. Bossi, H. Chen, P. De Camilli, P.P. Di Fiore, A single motif responsible for ubiquitin recognition and monoubiquitination in endocytic proteins, Nature 416 (2002) 451–455.
[21] S.C. Shih, D.J. Katzmann, J.D. Schnell, M. Sutanto, S.D. Emr, L. Hicke, Epsins and Vps27p/Hrs contain ubiquitin-binding domains that function in receptor endocytosis, Nat. Cell Biol. 4 (2002) 389–393.
[22] H. Barriere, C. Nemes, D. Lechardeur, M. Khan-Mohammad, K. Fruh, G.L. Lukacs, Molecular basis of oligoubiquitin-dependent internalization of membrane proteins in mammalian cells, Traffic 7 (2006) 282–297.
[23] H. Chen, S. Fre, V.I. Slepnev, M.R. Capua, K. Takei, M.H. Butler, P.P. Di Fiore, P. De Camilli, Epsin is an EH-domain-binding protein implicated in clathrin-mediated endocytosis, Nature 394 (1998) 793–797.
[24] I.G. Mills, G.J. Praefcke, Y. Vallis, B.J. Peter, L.E. Olesen, J.L. Gallop, P.J. Butler, P.R. Evans, H.T. McMahon, EpsinR: an AP1/clathrin interacting protein involved in vesicle trafficking, J. Cell Biol. 160 (2003) 213–222.
[25] J. Hirst, A. Motley, K. Harasaki, S.Y. Peak Chew, M.S. Robinson, EpsinR: an ENTH Domain-containing protein that interacts with AP-1, Mol. Biol. Cell 14 (2003) 625–641.
[26] C. Gabernet-Castello, J.B. Dacks, M.C. Field, The single ENTH-domain protein of trypanosomes; endocytic functions and evolutionary relationship with epsin, Traffic 10 (2009) 894–911.
[27] J.O. De Craene, R. Ripp, O. Lecompte, J.D. Thompson, O. Poch, S. Friant, Evolutionary analysis of the ENTH/ANTH/VHS protein superfamily reveals a coevolution between membrane trafficking and metabolism, BMC Genomics 13 (2012) 297.
[28] L. Kall, A. Krogh, E.L. Sonnhammer, Advantages of combined transmembrane topology and signal peptide prediction—the Phobius web server, Nucleic Acids Res. 35 (2007) W429–W432.
[29] T.N. Petersen, S. Brunak, G. von Heijne, H. Nielsen, SignalP 4.0: discriminating signal peptides from transmembrane regions, Nat. Methods 8 (2011) 785–786.
[30] K. Nakai, P. Horton, PSORT: a program for detecting sorting signals in proteins and predicting their subcellular localization, Trends Biochem. Sci. 24 (1999) 34–36.
[31] J.D. Thompson, D.G. Higgins, T.J. Gibson, CLUSTAL W: improving the sensitivity of progressive multiple sequence alignment through sequence weighting, position-specific gap penalties and weight matrix choice, Nucleic Acids Res. 22 (1994) 4673–4680.
[32] R. Koradi, M. Billeter, K. Wuthrich, MOLMOL: a program for display and analysis of macromolecular structures, J. Mol. Graph. 14 (1996) 51–55 (29–32).
[33] F. Melo, E. Feytmans, Assessing protein structures with a non-local atomic interaction energy, J. Mol. Biol. 277 (1998) 1141–1152.
[34] D. Eisenberg, R. Luthy, J.U. Bowie, VERIFY3D: assessment of protein models with three-dimensional profiles, Methods Enzymol. 277 (1997) 396–404.
[35] S.C. Lovell, I.W. Davis, W.B. Arendall III, P.I. de Bakker, J.M. Word, M.G. Prisant, J.S. Richardson, D.C. Richardson, Structure validation by Calpha geometry: phi, psi and Cbeta deviation, Proteins 50 (2003) 437–450.
[36] Y. Bromberg, G. Yachdav, B. Rost, SNAP predicts effect of mutations on protein function, Bioinformatics 24 (2008) 2397–2398.
[37] E. Gallego, M. Alvarado, M. Wasserman, Identification and expression of the protein ubiquitination system in *Giardia intestinalis*, Parasitol. Res. 101 (2007) 1–7.
[38] H.D. Lujan, M.R. Mowatt, J.T. Conrad, T.E. Nash, Increased expression of the molecular chaperone BiP/GRP78 during the differentiation of a primitive eukaryote, Biol. Cell. 86 (1996) 11–18.
[39] T.E. Nash, A. Aggarwal, R.D. Adam, J.T. Conrad, J.W. Merritt Jr., Antigenic variation in *Giardia lamblia*, J. Immunol. 141 (1988) 636–641.
[40] D.B. Keister, Axenic culture of *Giardia lamblia* in TYI-S-33 medium supplemented with bile, Trans. R. Soc. Trop. Med. Hyg. 77 (1983) 487–488.
[41] M.C. Touz, H.D. Lujan, S.F. Hayes, T.E. Nash, Sorting of encystation-specific cysteine protease to lysosome-like peripheral vacuoles in *Giardia lamblia* requires a conserved tyrosine-based motif, J. Biol. Chem. 278 (2003) 6420–6426.
[42] M.C. Touz, J.T. Conrad, T.E. Nash, A novel palmitoyl acyl transferase controls surface protein palmitoylation and cytotoxicity in *Giardia lamblia*, Mol. Microbiol. 58 (2005) 999–1011.
[43] H.G. Elmendorf, S.M. Singer, J. Pierce, J. Cowan, T.E. Nash, Initiator and upstream elements in the alpha2-tubulin promoter of *Giardia lamblia*, Mol. Biochem. Parasitol. 113 (2001) 157–169.
[44] S.M. Singer, J. Yee, T.E. Nash, Episomal and integrated maintenance of foreign DNA in *Giardia lamblia*, Mol. Biochem. Parasitol. 92 (1998) 59–69.
[45] J. Yee, T.E. Nash, Transient transfection and expression of firefly luciferase in *Giardia lamblia*, Proc. Natl. Acad. Sci. U. S. A. 92 (1995) 5615–5619.
[46] J. Li, B. Russell, Phosphatidylinositol 4,5-bisphosphate regulates CapZbeta1 and actin dynamics in response to mechanical strain, Am. J. Physiol. Heart Circ. Physiol. 305 (2013) H1614–H1623.
[47] H.D. Lujan, L.S. Diamond, Cholesterol requirement and metabolism in *Entamoeba histolytica*, Arch. Med. Res. 28 (1997) 96–97 (Spec No).
[48] S.E. Boucher, F.D. Gillin, Excystation of in vitro-derived *Giardia lamblia* cysts, Infect. Immun. 58 (1990) 3516–3522.

[49] M.R. Rivero, L. Kulakova, M.C. Touz, Long double-stranded RNA produces specific gene downregulation in *Giardia lamblia*, J. Parasitol. 96 (2010) 815–819.
[50] S.S. Cox, M. van der Giezen, S.J. Tarr, M.R. Crompton, J. Tovar, Evidence from bioinformatics, expression and inhibition studies of phosphoinositide-3 kinase signalling in *Giardia intestinalis*, BMC Microbiol. 6 (2006) 45.
[51] G. Di Paolo, P. De Camilli, Phosphoinositides in cell regulation and membrane dynamics, Nature 443 (2006) 651–657.
[52] R.J. Brady, Y. Wen, T.J. O'Halloran, The ENTH and C-terminal domains of *Dictyostelium epsin* cooperate to regulate the dynamic interaction with clathrin-coated pits, J. Cell Sci. 121 (2008) 3433–3444.
[53] P.B. Hylemon, H. Zhou, W.M. Pandak, S. Ren, G. Gil, P. Dent, Bile acids as regulatory molecules, J. Lipid Res. 50 (2009) 1509–1520.
[54] S. Hohenester, A. Gates, R. Wimmer, U. Beuers, M.S. Anwer, C. Rust, C.R. Webster, Phosphatidylinositol-3-kinase p110gamma contributes to bile salt-induced apoptosis in primary rat hepatocytes and human hepatoma cells, J. Hepatol. 53 (2010) 918–926.
[55] M.A. De Matteis, A. Di Campli, A. Godi, The role of the phosphoinositides at the Golgi complex, Biochim. Biophys. Acta 1744 (2005) 396–405.
[56] K. Hofmann, L. Falquet, A ubiquitin-interacting motif conserved in components of the proteasomal and lysosomal protein degradation systems, Trends Biochem. Sci. 26 (2001) 347–350.
[57] R.C. Aguilar, B. Wendland, Ubiquitin: not just for proteasomes anymore, Curr. Opin. Cell Biol. 15 (2003) 184–190.
[58] C. Faso, C. Konrad, E.M. Schraner, A.B. Hehl, Export of cyst wall material and Golgi organelle neogenesis in *Giardia lamblia* depend on endoplasmic reticulum exit sites, Cell. Microbiol. 15 (4) (2012) 537–553. http://dx.doi.org/10.1111/cmi.12054.
[59] D.S. Friend, The fine structure of *Giardia muris*, J. Cell Biol. 29 (1966) 317–332.
[60] V. Gaechter, E. Schraner, P. Wild, A.B. Hehl, The single dynamin family protein in the primitive protozoan *Giardia lamblia* is essential for stage conversion and endocytic transport, Traffic 9 (2008) 57–71.
[61] J.M. Turchany, J.M. McCaffery, S.B. Aley, F.D. Gillin, Ultrastructural effects of lactoferrin binding on *Giardia lamblia* trophozoites, J. Eukaryot. Microbiol. 44 (1997) 68–72.
[62] J.M. Turchany, S.B. Aley, F.D. Gillin, Giardicidal activity of lactoferrin and N-terminal peptides, Infect. Immun. 63 (1995) 4550–4552.
[63] J. Bittencourt-Silvestre, L. Lemgruber, W. de Souza, Encystation process of *Giardia lamblia*: morphological and regulatory aspects, Arch. Microbiol. 192 (2010) 259–265.
[64] J. Hyman, H. Chen, P.P. Di Fiore, P. De Camilli, A.T. Brunger, Epsin 1 undergoes nucleocytosolic shuttling and its eps15 interactor NH(2)-terminal homology (ENTH) domain, structurally similar to Armadillo and HEAT repeats, interacts with the transcription factor promyelocytic leukemia Zn(2) + finger protein (PLZF), J. Cell Biol. 149 (2000) 537–546.
[65] A. Sen, K. Madhivanan, D. Mukherjee, R.C. Aguilar, The epsin protein family: coordinators of endocytosis and signaling, Biomol. Concepts 3 (2012) 117–126.
[66] C.A. Horvath, D. Vanden Broeck, G.A. Boulet, J. Bogers, M.J. De Wolf, Epsin: inducing membrane curvature, Int. J. Biochem. Cell Biol. 39 (2007) 1765–1770.
[67] B. Ritter, P.S. McPherson, There's a GAP in the ENTH domain, Proc. Natl. Acad. Sci. U. S. A. 103 (2006) 3953–3954.
[68] Y. Hernandez, C. Castillo, S. Roychowdhury, A. Hehl, S.B. Aley, S. Das, Clathrin-dependent pathways and the cytoskeleton network are involved in ceramide endocytosis by a parasitic protozoan, *Giardia lamblia*, Int. J. Parasitol. 37 (2007) 21–32.
[69] M. Yichoy, E.S. Nakayasu, M. Shpak, C. Aguilar, S.B. Aley, I.C. Almeida, S. Das, Lipidomic analysis reveals that phosphatidylglycerol and phosphatidylethanolamine are newly generated phospholipids in an early-divergent protozoan, *Giardia lamblia*, Mol. Biochem. Parasitol. 165 (2009) 67–78.
[70] Y.A. Byekova, R.R. Powell, B.H. Welter, L.A. Temesvari, Localization of phosphatidylinositol (3,4,5)-trisphosphate to phagosomes in entamoeba histolytica achieved using glutathione S-transferase- and green fluorescent protein-tagged lipid biosensors, Infect. Immun. 3 (8) (2002) 513–520.
[71] K. Zhou, S. Pandol, G. Bokoch, A.E. Traynor-Kaplan, Disruption of Dictyostelium PI3K genes reduces [32P]phosphatidylinositol 3,4 bisphosphate and [32P]phosphatidylinositol trisphosphate levels, alters F-actin distribution and impairs pinocytosis, J. Cell Sci. 111 (Pt 2) (1998) 283–294.
[72] V. Legendre-Guillemin, S. Wasiak, N.K. Hussain, A. Angers, P.S. McPherson, ENTH/ANTH proteins and clathrin-mediated membrane budding, J. Cell Sci. 117 (2004) 9–18.
[73] B. Wendland, Epsins: adaptors in endocytosis? Nat. Rev. Mol. Cell Biol. 3 (2002) 971–977.
[74] E.M. Lafer, Clathrin–protein interactions, Traffic 3 (2002) 513–520.
[75] M.T. Drake, M.A. Downs, L.M. Traub, Epsin binds to clathrin by associating directly with the clathrin-terminal domain. Evidence for cooperative binding through two discrete sites, J. Biol. Chem. 275 (2000) 6479–6489.
[76] J.A. Rosenthal, H. Chen, V.I. Slepnev, L. Pellegrini, A.E. Salcini, P.P. Di Fiore, P. De Camilli, The epsins define a family of proteins that interact with components of the clathrin coat and contain a new protein module, J. Biol. Chem. 274 (1999) 33959–33965.
[77] M.T. Drake, L.M. Traub, Interaction of two structurally distinct sequence types with the clathrin terminal domain beta-propeller, J. Biol. Chem. 276 (2001) 28700–28709.
[78] M.C. Touz, The unique endosomal/lysosomal system of *Giardia lamblia*, in: B. Ceresa (Ed.), Molecular Regulation of Endocytosis, vol. 1, InTech, Croatia, 2012 (pp. http://www.intechopen.com/books/molecular-regulation-of-endocytosis/the-unique-endosomal-lysosomal-system-of-giardia-lamblia).
[79] C.A. Nino, J. Chaparro, P. Soffientini, S. Polo, M. Wasserman, Ubiquitination dynamics in the early-branching eukaryote *Giardia intestinalis*, Microbiologyopen 2 (2013) 525–539.
[80] C. Kalthoff, S. Groos, R. Kohl, S. Mahrhold, E.J. Ungewickell, Clint: a novel clathrin-binding ENTH-domain protein at the Golgi, Mol. Biol. Cell 13 (2002) 4060–4073.
[81] L. Eckmann, Mucosal defences against Giardia, Parasite Immunol. 25 (2003) 259–270.
[82] R. Jiang, V. Lopez, S.L. Kelleher, B. Lonnerdal, Apo- and holo-lactoferrin are both internalized by lactoferrin receptor via clathrin-mediated endocytosis but differentially affect ERK-signaling and cell proliferation in Caco-2 cells, J. Cell. Physiol. 226 (2011) 3022–3031.
[83] M. Huettinger, H. Retzek, M. Hermann, H. Goldenberg, Lactoferrin specifically inhibits endocytosis of chylomicron remnants but not alpha-macroglobulin, J. Biol. Chem. 267 (1992) 18551–18557.
[84] J.A. Fresno Vara, E. Casado, J. de Castro, P. Cejas, C. Belda-Iniesta, M. Gonzalez-Baron, PI3K/Akt signalling pathway and cancer, Cancer Treat. Rev. 30 (2004) 193–204.
[85] M. Benchimol, *Giardia lamblia*: behavior of the nuclear envelope, Parasitol. Res. 94 (2004) 254–264.
[86] E.J. Tran, S.R. Wente, Dynamic nuclear pore complexes: life on the edge, Cell 125 (2006) 1041–1053.
[87] P. Tumova, K. Hofstetrova, E. Nohynkova, O. Hovorka, J. Kral, Cytogenetic evidence for diversity of two nuclei within a single diplomonad cell of Giardia, Chromosoma 116 (2007) 65–78.
[88] A.A. Saraiya, C.C. Wang, snoRNA, a novel precursor of microRNA in *Giardia lamblia*, PLoS Pathog. 4 (2008) e1000224.
[89] J.A. Ebneter, A.B. Hehl, The single epsin homolog in *Giardia lamblia* localizes to the ventral disk of trophozoites and is not associated with clathrin membrane coats, Mol. Biochem. Parasitol. 197 (1–2) (2014) 21–27. http://dx.doi.org/10.1016/j.molbiopara.2014.09.008.